Development of heat shock resistance in *L. pneumophila* modeled by experimental evolution

Jeffrey Liang[1], Sebastien P. Faucher[1,2]

1. Department of Natural Resource Sciences, McGill University, Sainte-Anne-de-Bellevue, Québec, Canada
2. Centre de Recherche en Infectiologie Porcine et Avicole (CRIPA), Faculté de Médecine Vétérinaire, Université de Montréal, Saint-Hyacinthe, QC, Canada

Corresponding author: Sebastien P. Faucher sebastien.faucher2@mcgill.ca

Running title: Heat-shock Evolution in *Legionella pneumophila*

Abstract

Because it can grow in buildings with complex hot water distribution systems (HWDS), healthcare facilities recognize the waterborne bacterium *Legionella pneumophila* as a major nosocomial infection threat and often try to clear the systems with a pasteurization process known as superheat-and-flush. After this treatment, many facilities find that the contaminating populations slowly recover, suggesting the possibility of *in situ* evolution favouring increased survival in high temperature conditions. To mimic this process in a controlled environment, an adaptive laboratory evolution (ALE) model was used to select a wild-type strain of *L. pneumophila* for survival to transient exposures to temperatures characteristic of routine hot water use or failed pasteurization processes in HWDS. Over their evolution, these populations became insensitive to exposure to 55 °C and innovated the ability to survive short exposures to 59 °C heat shock. Heat-adapted lineages maintained a higher expression of heat shock genes during low-temperature incubation in freshwater, suggesting a pre-adaptation to heat stress. Although there were distinct mutation profiles in each of the heat-adapted lineages, each acquired multiple mutations in the DnaJ/DnaK/ClpB disaggregase complex, as well as mutations in chaperone *htpG* and protease *clpX.* These mutations were specific to heat shock survival and were not seen in control lineages included in the ALE without exposure to heat shock. This study supports *in situ* observations of adaptation to heat stress and demonstrate the potential of *L. pneumophila* to develop resistance to control measures.

Importance

As a bacterium that thrives in warm water ecosystems, *Legionella pneumophila* is a key factor motivating regulations on hot water systems. Two major measures intended to control *Legionella* are the maintenance of high circulating temperatures to curtail growth and the use of superheat-and-flush pasteurization processes to eliminate established populations. Although hospitals are particularly vulnerable to nosocomial pneumoniae caused by *Legionella*, they recurrently experience recolonization

of their hot water systems after treatment. To understand these long-term survivors, we have used an experimental evolution model to replicate this process. We find major differences between the mutational profiles of heat-adapted and heat-naïve *L. pneumophila* populations, including mutations in major heat shock genes like chaperones and proteases. This model demonstrates the value of appropriate heat treatment of *L. pneumophila* contaminated systems and – in an analogue to antibiotic resistance – the importance of complete eradication of the resident population to prevent selection for more persistent bacteria.

Key words: Legionella pneumophila, Hot water distribution systems, Adaptive laboratory evolution, Experimental evolution, Heat resistance, Pasteurization

46 # Introduction

47 As an obligate intracellular pathogen, the bacterium *Legionella pneumophila* relies on infection of
48 eukaryotic cells in order to acquire nutrients and replicate (1). Though it usually lives in freshwater
49 ecosystems where it targets free-living eukaryotic hosts from diverse clades, *L. pneumophila* is now also
50 known to infect humans where it targets alveolar macrophages (2). Its contamination of human-built
51 infrastructure favours infection by aerosolizing the bacteria and facilitating its travel into the lungs (2, 3).
52 Globally, *L. pneumophila* is the main cause of Legionnaires' Disease, a life-threatening pneumonia whose
53 severity and under-diagnosis have led to its high overall case-fatality rate, estimated at between 5 and
54 10%, with even higher death rates for nosocomial cases (4–6). Early suspicions focused on dispersal
55 through contaminated cooling tower emissions (7, 8), but *L. pneumophila* has since been found in diverse
56 engineered water systems, including in whirlpool spas, decorative fountains, and – significantly for
57 nosocomial infection – in hospital plumbing systems (9).

58 The engineering of water systems has a major impact on the growth potential of *L. pneumophila* (10, 11).
59 Large buildings with complex plumbing systems are particularly vulnerable to contamination, and studies
60 have shown that multiple clades of *L. pneumophila* can stably co-exist in these systems (12). As a
61 mesophilic bacterium which replicates best between 20 and 45 °C (13), *L. pneumophila* favours
62 colonization of hot water distribution systems (HWDS). Deprecated fixtures, as well as the improper
63 design of plumbing networks or incorrect estimation of water demand, can lead to stagnation and the
64 existence of dead legs. These regions of low water flow allow scale and biofilms to accumulate – physical
65 structures that can physically protect *Legionella* from exposure to disinfectants (14, 15). Policies that
66 decrease water temperatures in favour of energy savings can result in tepid temperatures that favour the
67 growth *L. pneumophila* and of its eukaryotic hosts (16, 17). Hospitals are particularly at risk both because
68 they must balance hot water temperatures against the risks of scalding and because they often house

69 immunocompromised patients who are particularly threatened by exposure to recurrent bacterial
70 contaminants (18, 19).

71 Along with chemical treatment via chlorination or copper-silver ionization, the maintenance of high-
72 temperatures along the length of a plumbing system from the water heater through to the terminal
73 outlets is a critical control measure against *L. pneumophila* (20). Remedial high-temperature
74 pasteurization processes, collectively termed superheat-and-flush, aim to push hot water temperatures
75 above what *L. pneumophila* can tolerate (21, 22). The implementation of these strategies can differ
76 depending on the specific architecture of the HWDS, but they aim to raise temperatures throughout the
77 entire system through to the distal outlets. Though remedial pasteurization can be effective at the short-
78 term clearance of *Legionella*, longitudinal studies have shown that re-contamination is common over
79 month or year-long time scales (23–25). It has been reported that repeated use of high-temperature
80 pasteurization to disinfect these water systems can instead lead to the local evolution of more heat
81 resistant *L. pneumophila* populations, like the familiar phenomenon of antibiotic tolerance (20, 22, 23).

82 In bacteria, heat stress can damage several vital subcomponents of the cell by causing membrane
83 depolarization and damage, destabilization of the nucleoid, and the inactivation and aggregation of vital
84 enzymes and structural proteins (26–28). Bacteria have developed a sophisticated heat shock response,
85 centralized through the alternative sigma factor RpoH that redirects transcription towards stress
86 resistance by driving the production of heat shock proteins (29, 30). These heat shock proteins buffer the
87 toxic effects of misfolded and aggregated proteins in the cell – either by promoting refolding or by
88 targeting them for destruction (31, 32). These proteins are broadly conserved among bacterial species
89 and include proteases as well as chaperones, such as HtpG and DnaK, and their co-chaperone proteins,
90 such as DnaJ and GrpE. After the thermal shock is resolved, these proteins are also involved in a negative
91 feedback loop targeting RpoH for destruction by FtsH, a membrane-bound protease (33, 34). This
92 organization is conserved in *L. pneumophila*, with five heat shock proteins identified in radiolabelling

93 studies (35) and many more annotated from the published genetic sequence (36, 37). Heat shock proteins
94 are also involved in the early pathogenesis in *L. pneumophila* by promoting the internalization of the
95 bacterium by the host cell and reorganizing host trafficking processes (38–40). The LetAS and CpxRA two-
96 component systems are also known to influence heat shock survival, likely mediated through their
97 regulation of life phase switching during growth and starvation (41, 42).

98 Adaptive laboratory evolution (ALE) is an experimental concept that manipulates a chosen organism in a
99 laboratory setting to providing insights into complicated phenomena from the wild (43, 44). To simulate
100 long-term exposure to high temperatures in HWDS, we can depend on the short generation times and the
101 relative ease of culture and storage of *L. pneumophila* in laboratory conditions to study the resulting
102 evolution in a controlled and repeatable process. ALE has been applied in numerous bacterial and non-
103 bacterial species to study the trajectories and repeatability of evolutionary responses without *a priori*
104 expectations on the loci which will be targeted (45, 46). Prior studies have used ALE to adapt *Escherichia*
105 *coli* to growth in stably high-temperature or low pH conditions, as well as to survival acute population
106 bottlenecking by ionizing radiation (47–49). Notable ALE experiments conducted with *L. pneumophila*
107 have been used to study resistance to fluoroquinolone and macrolide antibiotics (50, 51) and adaptation
108 to mouse macrophages (52). As heat stress non-specifically challenges multiple components of the
109 bacterial cell, ALE makes an appropriate protocol to study the range of mutations driving the increasing
110 heat tolerance of *L. pneumophila* populations observed in hot water systems.

111 To bridge the gap between *in situ* observations of *L. pneumophila*'s adaptation to pasteurization in HWDS
112 and an understanding of its underlying genetic mechanisms, we tailored an ALE study design to investigate
113 the evolutionary paths that the environmental pathogen can take to develop a tolerance of heat shock.
114 The aim was to document the genetic changes that surviving population would develop under transient
115 exposure to high temperatures, simulating failed pasteurizations or bursts of hot water from routine
116 outlet use. We report that ALE can reliably induce resistance to heat shock in adapted lineages through

117 underlying mutations that cause differences both in transcriptional regulation and heat shock protein
118 activity. In our model, adaptation to heat shock resulted in no fitness deficits during axenic or infectious
119 growth, supporting epidemiological studies that connect HWDS isolates to clinical isolates from exposed
120 individuals.

121 # Results

122 Studies tracking the population structure over time of *L. pneumophila* growing in HWDS have repeatedly
123 confirmed that persistence and microevolution is more common than recontamination from the incoming
124 water supply. Even more troubling, repeated exposure to high temperatures through bursts of hot water
125 demand or failed cycles of superheat-and-flush are liable to favour heat resistance in the surviving
126 bacteria. To simulate this process and study it in a controlled environment, we designed an adaptive
127 evolution system to simulate transient and sublethal exposures to high temperatures. Based on pilot data
128 and typical global public health recommendations (13), we exposed the study populations to 55 °C by
129 immersion in a circulating water bath for 15 minutes, as described in Materials and Methods. We
130 maintained six replicate lineages of the wild-type Philadelphia-1 strain to determine the replicability of
131 our evolutionary pathways under heat shock (Figure 1A). In parallel, we also maintained six replicate
132 control lineages to compensate for mutations that favour growth in laboratory conditions and isolate the
133 changes related to heat shock (Figure 1B). Bacterial population sizes were bottlenecked at each cycle by
134 either selection for survivors of heat shock or by sub-sampling of control populations suspended in
135 freshwater.

136 Over the 70 cycles of the ALE protocol, we raised the heat shock temperature on an *ad hoc* basis to
137 maintain a stable level of population loss in the heat adapted lineages from 55 °C at the beginning of the
138 experiment to 59 °C at its conclusion (Figure 1C). The resulting six heat-adapted populations were named
139 HA-1 through HA-6 and the six control lineages were named C-1 through C-6 (Table 1). Whole genome
140 sequencing revealed that HA-4 had been contaminated by HA-6 by the end of the experiment, so it was
141 removed from final analysis. Regardless, all replicate heat adapted lineages showed a robust increase in
142 heat shock resistance when challenged by heat shock for 20 minutes (Figure 1C). The decimal reduction
143 time required to reduce the initial populations by 90% increased from 303 seconds at 55 °C at the outset

144 of the ALE to a minimum of 9546 seconds by passage 6 (Figure 1C). After 65 and 70 cycles of selection,
145 there was no significant population drop even after a 30-minute exposure. After 20 and 65 passages
146 respectively, populations could survive 57 °C and 59 °C for 20 minutes. In contrast, neither the control
147 lineages nor the ancestral strain was able to tolerate 57 °C for 20 minutes (data not shown).

148 Despite their acquired ability to tolerate heat shock, the heat adapted lineages did not lose the ability to
149 grow axenically or in host cells. We directly competed the evolved lineages against their ancestral strain
150 by growing them together in co-culture to test for relative fitness. Plasmids pXDC31 and pMMB207c,
151 which differ only in that pXDC31 has an IPTG-inducible *gfp* insert, were used to distinguish between
152 strains. Both plasmids were electroporated into the Philadelphia-1 ancestor as well as Passage 70
153 populations of both HA-1 and C-1 and transformed isolates were used in the competition experiments. To
154 control for possible fitness confounds introduced by the plasmid inserts, all pairs were tested with a
155 reciprocal expression of *gfp* in both competitors (e.g., HA-1 pXDC31 was competed against Philadelphia-
156 1 pMMB207C and HA-1 pMMB207C was competed against Philadelphia-1 pXDC31). Control competitions
157 of HA-1 and C-1 with themselves showed a neutral relative fitness, as expected ($p = 0.4123, 0.5233$).
158 Both ALE-derived competitors were also at neutral relative fitness against each other ($p =$
159 $0.0547, 0.2113$), indicating that both were equally well adapted to growth in AYE. In contrast,
160 Philadelphia-1 was significantly less fit than either HA-1 ($p = 0.0120, 0.0235$) or C-1 ($p =$
161 $0.0090, 0.0244$), supporting our hypothesis that the populations would evolve better growth in AYE in
162 tandem with heat resistance. To test whether this increased growth potential in AYE was replicated during
163 host cell infection, we tested for three-day bacterial yield after growth in the amoeba *V. vermiformis*.
164 Consistent with a specific adaptation to growth in cell-free conditions, replication of the heat-adapted
165 lineages did not significantly differ from those of Philadelphia-1 or the control lineage (Figure 1E).

166 Because the early bacterial heat shock response relies largely on a re-direction of transcription by the
167 *rpoH* sigma factor, we expected that there would be a difference in RNA expression profiles between our

168 heat-adapted, control, and ancestral strains. To represent the regulators and effectors of the
169 transcriptional heat shock response, we measured differential expression of three sigma factors and 7
170 heat shock proteins. These were chosen to represent genes likely to be involved in the heat shock
171 response, as well as those mutated in multiple lineages under heat shock selection. Upon heat shock, the
172 ancestor Philadelphia-1 displays significant up-regulation in *clpB*, *dnaJ*, *dnaK*, *groL*, and *htpG* expression
173 but not of *clpX*, *lon*, or *phaP* by two-way ANOVA (Figure 2 A). Similarly, *rpoH* is the only sigma factor whose
174 RNA levels are elevated (Figure 2B). Compared to Philadelphia-1, the heat-adapted lineages (and to a
175 lesser extent, the control lineages) over-express heat shock protein mRNAs prior to heat shock exposure
176 (Figure 2C). This over-expression is no longer seen when comparing expression profiles after heat shock,
177 suggesting a pre-adaptation to thermal stress in chronically heat-exposed populations (Figure 2D).

178 To identify the mutations acquired after 70 cycles of the ALE, we used Breseq, a pipeline designed for the
179 analysis of short read data from bacterial evolution experiments. To capture the population diversity, we
180 isolated 10 clones from each heat-adapted lineage and 5 clones from each control lineage for whole-
181 genome sequencing. As described in Materials and Methods, per-isolate analysis of the sequence reads
182 showed gaps of missing coverage, so reads from the replicate clones of each lineage were pooled and re-
183 analysed in the polymorphism setting of Breseq to measure allele frequency of novel mutations. Re-
184 sequencing of our Philadelphia-1 strain showed that it differs from the published genome (CP015927.1)
185 by the absence of a 38 kbp island pPh38 and by a missense mutation in the *letA* gene (Table 3). Genes
186 mutated in replicate heat-adapted lineages included multiple heat shock genes (*htpG*, *clpB*, *clpX*, *dnaJ*,
187 and *dnaK*), as well as lpg0563 (*phaP*), lpg2351 (*mavF*), and genes associated with cell wall synthesis (*mreC*
188 and *rodA*) (Figure 3 and Table 3). A separate mutation profile was seen in the replicate control lineages,
189 with multiple hits in *nusG*, *rpoB*, *cpxR*, and *lidA* (Figure 3). Each lineage displayed a unique mutational
190 profile, showing that *L. pneumophila* can follow multiple evolutionary pathways to acquire strong heat
191 resistance (Supplementary table 1).

192 The *L. pneumophila* homologue of *htpG* (bacterial 90 kilodalton heat shock protein) acquired mutations
193 in three of the heat-adapted lineages including a nonsense mutation in HA-5 (Q148*) and a frameshift
194 mutation in HA-6 (del1bp 503). Sequencing of HA-4 after 30 passages (before it had been contaminated)
195 also showed a third distinct loss-of-function mutation (del1bp 694) (Supplementary table 2). Though
196 surprising for a known heat shock protein, this was consistent with our prior finding that a deletion mutant
197 lacking *htpG* showed increased survival under heat stress. Western blotting confirmed that the typical
198 HtpG protein was not produced in HA-5 or HA-6, while the missense mutation (G83E) in HA-3 did not
199 affect antibody binding (Figure 4A). The *htpG* alleles found in HA-3, HA-5 and HA6 were mobilized into the
200 chromosome of the lab strain KS79 by allelic exchange in tandem with a selectable marker. Phenotypically,
201 the mutant alleles of *htpG* raised heat shock resistance in *L. pneumophila* to a similar magnitude as the
202 previously constructed full deletion mutant (Figure 4B). Reciprocally, none of the mutant alleles were able
203 to complement the raised heat resistance of the deletion mutant (Figure 4C).

204 To test whether *htpG* mutation was favoured only due to its role in heat shock, we constructed a
205 competition assay to compare the growth of KS79 and of the deletion mutant against the mutant
206 harbouring the different alleles of *htpG* (Figure 4D). The wild-type KS79 under-competed against any
207 strain containing a blank plasmid or plasmid carrying any derived allele of *htpG*. Conversely, it was
208 neutrally fit against the *htpG* mutant complemented with a wild-type allele of *htpG*. KS79 and the deletion
209 mutant both grew significantly better in the presence of competitors harbouring the ancestral allele of
210 *htpG* compared to competitors harbouring a blank plasmid, suggesting that HtpG, in addition to conferring
211 reduced heat shock resistance, may also reduce growth potential in AYE.

212 # Discussion

213 ## *L. pneumophila* rapidly adapts to repeated exposure to heat shock

214 As an opportunistic colonizer of plumbing infrastructure, *L. pneumophila* is commonly recognized as a
215 major hazard under the purview of hospital facilities managers (18). To model its long-term residence in
216 hot water systems, our system of laboratory evolution was able to robustly raise the heat tolerance levels
217 of wild-type *L. pneumophila*. The lineages' survival of 55 °C – a commonly recommended circulation
218 temperature (53, 54) – highlights the scale of their adaptation. Prior to their passage through the ALE
219 model, the ancestral strain could survive only 5 minutes of exposure to this temperature before suffering
220 a population reduction of 90% (Figure 1C). After 65 rounds of selection, the heat-adapted lineages could
221 sustain exposure to the same temperature for at least 30 minutes without showing significant population
222 loss. The final selection condition – 15 minutes at 59 °C – was much more intense that what the ancestral
223 strain could survive and indeed our control lineages, which were also tested for heat shock survival,
224 consistently failed to survive temperatures of 57 °C and higher.

225 A major concern underlying our experiment was that *L. pneumophila*, accustomed to replication inside
226 eukaryotes, would simultaneously favour adaptation towards growth in liquid media and lose the ability
227 to replicate inside host cells. We included replicate control lineages to anticipate the changes that might
228 be seen after repeated growth in AYE. Testing populations from both branches of the evolution
229 experiment, we found that both branches of the experiment retained their ancestral ability to replicate
230 inside *V. vermamoeba* (Figure 1E). On the other hand, passage in axenic culture significantly elevated the
231 relative fitnesses of both the control and heat-adapted lineages in AYE culture compared to Philadelphia-
232 1 (Figure 1D). Despite relaxed constraints during the selection of the control lineage, the heat-adapted
233 lineage had an equal ability to grow in AYE or inside host amoeba without needing to trade-off the ability
234 to tolerate heat shock.

235 ## Tandem adaptation of transcription and translation during adaptation to axenic culture

236 Consistent with their separate evolutionary pressures, the control and heat-adapted lineages adopted
237 divergent evolutionary patterns. RNA transcription genes *nusG* and *rpoB* (55, 56) were both non-
238 synonymously mutated in multiple control lineages, as was the S10 ribosomal protein *nusE* (Table 3 and
239 Figure 3). RpoB is the beta-subunit of the RNA polymerase (RNAP) complex and is commonly mutated in
240 bacterial evolution studies in diverse contexts including acid resistance, ionizing radiation, and
241 atmospheric pollution (47, 49, 57). Four different missense mutations in *rpoB* were independently fixed
242 in two control lineages (G759E and N1350T) and in two heat-adapted lineages (G138E and K924N). The
243 transcription factor NusG binds to the RpoB through its N-terminal domain and to NusE through its C-
244 terminal domain, coupling transcription to translation (55, 58). The two mutations seen in NusG (R136I
245 and V143D) both sit within the C-terminal KOW domain (59) and are in lineages C-2 and C-6 – mutually
246 exclusive with mutations in *rpoB* and *nusE* harboured in lineages C-4 and C-5. NusG enhances both RNAP
247 processivity and rho-dependent termination, so the partition of these mutations could suggest
248 incompatibility between the NusG and RpoB/NusE mutations, though epistasis was not tested in this study
249 (55, 56, 60). From ALE experiments in *E. coli,* mutations in *rpoB* are known to cause broad changes to
250 global transcription (61) and can optimize replication rates during exponential growth (62, 63). In these
251 experiments, the same mutations in *rpoB* that contribute to faster exponential growth rates also reduce
252 the ability of these strains to tolerate acid shock and antibiotic exposure (63). This may explain the
253 distinction between the *rpoB* mutations found in the heat-adapted and control lineages, as heat shock
254 similarly induces a hostile environmental change. The two-component system response regulator *cpxR*
255 was mutated in three lineages in the control arm, but in none of the heat-adapted lineages. Of the three
256 distinct mutations, two were conversions of aspartic acid to asparagine (D190N and D194N) in the
257 OmpR/PhoB-type DNA binding domain (64, 65). This system is involved in controlling the expression of
258 Type II and Type IV secretion system genes and the control of virulence during the switch between

259 exponential and post-exponential phases (66, 67). Prior work in our lab has shown that *cpxR* is necessary
260 for heat shock tolerance (42) – this could underlie an evolutionary inelasticity that favours its mutation in
261 control lineages but not in heat-adapted lineages.

262 Central role of the DnaJ/DnaK/ClpB disaggregase complex in heat shock adaptation

263 Adaptation to heat stress, as expected, took multiple unique but overlapping pathways. Canonical heat
264 shock factors were common targets of mutation, and included *htpG, clpB*, *clpX*, *dnaJ*, and *dnaK*. These are,
265 variously, chaperone and co-chaperone proteins that act on misfolded and aggregated proteins to resolve
266 the effects of protein damage (68). The *bona fide* HSP40 co-chaperone *dnaJ* was mutated in all five heat-
267 adapted lineages, while neither of the HSP40 homologues *cbpA* or *djlA* (69–71) received any mutations.
268 Four distinct mutations were acquired in *dnaJ*, including three missense mutations and a single nucleotide
269 insertion. Three mutations – P334S, R318T, and an insertion at nucleotide 1100 (codon 337) – are in the
270 C-terminal end of the polypeptide. This region has been linked to the binding between DnaJ and DksA, a
271 regulator of RNA polymerase and the stringent response which influences heat shock resistance in *L.*
272 *pneumophila* (72–75). Autodimerization and chaperone functions in DnaJ also involve this C-terminal
273 region (76). Two lineages derived the same mutation – F95Y – in a linker region connecting the J-domain
274 and central zinc-binding regions of DnaJ. This phenylalanine position is conserved across bacterial and
275 eukaryotic homologues of DnaJ as a residue in the first of three DIF (DVF in *Legionella*) motifs (77).
276 Experimental substitution of this residue in *E. coli* causes a growth defect at low temperatures but has no
277 effect on high-temperature growth or on motility. The integrity of this glycine-phenylalanine rich region
278 is thought to be involved in proper DnaK/DnaJ ATP cycling and substrate release (77). This mutation in
279 DnaJ may contribute to the constitutively high expression of heat shock genes seen in our heat adapted
280 lineages by causing an accumulation of DnaK-substrate complexes and causing a de-repression of steady
281 state *rpoH* mRNA levels (78).

282 DnaK, a bacterial HSP70 and collaborator with DnaJ in protein refolding, acquired the same mutation in
283 three lineages – M94I. Both F95Y mutations in DnaJ were coincident with this DnaK allele, with HA-2 also
284 possessing a second V373L missense mutation in DnaK. These mutations both alter residues exposed on
285 the AlphaFold predicted surface of the DnaK protein (79, 80), suggesting that their effects lie in
286 modification of the substrate binding or co-chaperone dynamics of the heat shock response network. The
287 DnaK/DnaJ chaperone-co-chaperone system also interacts with ClpB, or HSP100, a AAA+ ATPase with
288 homologue found in all three domains of life (81–83). In various species of bacteria, ClpB assists in the
289 tolerance of high temperatures, ethanol damage, and oxidative stress by acting as a disaggregase of
290 tangled polypeptides (81). Its proper function depends on the assembly of an active hexamer from ClpB
291 monomers, forming a central channel that the misfolded substrate is threaded through. Interaction with
292 DnaK, as well as hexameric assembly of the protein complex, depends on the M-domain of ClpB (84, 85).
293 This section of the larger AAA+ domain includes four surface-exposed α-helices and spans the two
294 mutations observed in ClpB (A478V and A492T). The presumed effect of these mutations is to influence
295 protein-protein interactions either during self-hexamerization or when interfacing with DnaK (86, 87).

296 Refinement of the heat shock response by protein degradation

297 A second hexameric AAA+ ATPase, ClpX, also showed signs of adaptation with mutations in two lineages
298 targeting adjacent residues – G202A and E203D. Unlike ClpB, ClpX favours proteolysis over refoldase
299 activity, acting in concert with the peptidase ClpP (88). The two mutated residues are both in the AAA+
300 domain of ClpX and may allow for a refinement of the proteolytic capacity of *L. pneumophila* that
301 remediates the enrichment of unfolded and aggregated protein precipitated by high temperature
302 exposure.

303 As we had previously observed (75), the 90 kilodalton heat shock protein HtpG has an unlikely role in the
304 heat resistance of *L. pneumophila*. Its up-regulation after heat shock, role in high temperature growth in

305 other species, and its chaperone function all strongly support its identity as a heat shock protein (89–91),
306 but the deletion of *htpG* from a wild-type background increases the ability of *L. pneumophila* to survive
307 exposure to 55 °C for 15 minutes. This is further corroborated by the observed mutations in the ALE, with
308 three different mutations observed in three of the heat-adapted lineages. Two of these mutations –
309 Q148* in HA-5 and a single base pair deletion at position 503 in HA-6 – abrogate the structure of the
310 chaperone, leading to the loss of recognition by an anti-HtpG antibody. These three alleles provide the
311 same resistance to heat shock as the full deletion of *htpG*, and do not complement the deletion. We
312 hypothesized that these presumed loss of function mutations may give a growth advantage between heat
313 shock bottlenecks. We tested this in a relative fitness experiment measuring the growth of a deletion
314 mutant heterologously expressing the wild-type and derived alleles of *htpG*. Strains lacking *htpG* were
315 more relatively fit than one expressing wild-type *htpG*. This was also true for all three derived alleles of
316 *htpG*; the loss of HtpG function during the ALE could therefore have promoted both increased growth in
317 AYE and survival under heat shock. As *htpG* mutations were only seen in our heat-adapted lineages, it
318 seems likely that the increase in heat resistance is the more significant factor favouring their selection.

319 Mutations in virulence factors

320 Strikingly, the *lidA* gene was mutated singly or doubly in each of the six control lineages but in none of the
321 heat-adapted lineages. Each lineage acquired either one of two frameshift mutations (single base
322 deletions at nucleotides 1122 or 1566) or a premature stop (E508*). LidA is a Rab GTPase-binding effector
323 protein trafficked into the host cell by Icm/Dot Type IVb secretion system whose role in infection seems
324 largely involve disruption of the host trafficking system (92, 93). The role that these mutations in *lidA* play
325 in this evolutionary system is obscure considering that (i) the ALE was carried out without passage through
326 host cells, (ii) effector proteins are thought to be highly redundant and the repeated mutation of *lidA* is *a*
327 *priori* unexplained, and (iii) *lidA* mutation seems to have been highly selected for in control lineages but
328 disfavoured during heat-adaptation. The study which characterized *lidA* found that its absence caused the

329 Icm/Dot complex to become toxic to the bacterium, which was attributed to a possible toxic increase of
330 solute permeability (94). An increase of permeability following the loss of LidA may support increased
331 nutrient uptake in AYE, though the factors favouring complete saturation of *lidA* mutations across all the
332 control lineages and none of the heat-adapted ones remain unclear.

333 Loss-of-function mutations were a recurrent process across both branches of the ALE with lpg0563 (*phaP*)
334 and *mavF* also acquiring frameshift indels in multiple heat-adapted lineages. Each of the five heat-adapted
335 lineages acquired one of two distinct null mutations in *mavF* – a single base pair deletion of nucleotide
336 368 or a single base pair insertion at position 456. The biological mechanism favouring this mutation is
337 difficult to deduce as the protein is translocated through the Icm/Dot system and therefore likely no *prima*
338 *facie* relevance to heat shock survival in the absence of host cells (95).

339 Future avenues

340 With hospitals recognizing the dangers that *L. pneumophila* introduces when it contaminates their HWDS
341 plumbing, it is important to understand its life in these systems before it causes nosocomial infection.
342 Heat-based control measures are common, but *L. pneumophila* is often able to survive both routine hot
343 water temperature regimes and remedial superheat-and-flush interventions (23, 96). Our ALE model of *L.*
344 *pneumophila* microevolution under selective pressure from transient heat shock shows that it can follow
345 several separate evolutionary pathways to acquire heat resistance and replicates *in situ* studies that find
346 increased heat resistance in isolates taken after failed heat treatment (23). *L. pneumophila* lineages in this
347 system evolved in isolation from the broader HWDS microbiome. Even without these exogenous sources
348 of novel DNA, these populations evolved under the pressure of heat shock to survive up to 59 °C. These
349 mutations were concentrated both in well-known chaperones and proteases (*dnaJ*, *dnaK*, *clpX*, etc.), as
350 well as in unexpected proteins with unrelated functions (*phaP*, *mavF*, etc.). This model helps inform our
351 understanding of the forces operating on *L. pneumophila* in hot water plumbing and provides a platform

352 for future work to directly confirm the biological significance of the genetic changes that we have

353 observed in this study.

354 # Materials and Methods

355 ## Routine culture methods

356 *L. pneumophila* strains were routinely grown from frozen stocks stored at -80 °C on CYE (ACES-buffered
357 charcoal yeast extract) agar plates (Sigma-Aldrich) adjusted to pH 6.90 with KOH and supplemented with
358 0.25 g/L L-cysteine and 0.4 g/L ferric pyrophosphate and incubated at 37 °C for 72 hours. Single colonies
359 were sub-cultured into AYE broth (CYE without charcoal or agar) and grown shaking at 37 °C overnight. To
360 simulate residence in tap water, Fraquil, a defined low-nutrient medium (97) that simulates freshwater
361 was used to suspend *L. pneumophila*. *E. coli* strain DH5α was grown in LB agar or broth, as indicated, at
362 37 °C overnight. Where required, media was supplemented with 5 mg/L (*L. pneumophila*) or 25 mg/L (*E.*
363 *coli*) chloramphenicol, 25 mg/L kanamycin sulfate and/or 0.1 mM isopropyl β-d-1-thiogalactopyranoside
364 (IPTG). The strains used in this study are listed in Table 1. *Vermamoeba vermiformis* was maintained in
365 modified PYNFH (ATCC media 1034) at room temperature (20-28 °C) and passaged once per week (42).

366 ## Adaptive laboratory evolution procedure

367 The adaptive laboratory evolution experiment was designed with two arms deriving from one common
368 ancestral strain. *L. pneumophila* str. Philadelphia-1 (ATCC 33152) was obtained from the American Type
369 Culture Collection; it is a clinical isolate collected from the 1976 outbreak of Legionnaires' Disease in
370 Philadelphia. Because this isolate was sourced from a cooling tower, we expected it to be poorly adapted
371 to growth in laboratory conditions in axenic medium, a known selection pressure in ALE experiments. To
372 account for this, we included both an experimental arm which was exposed to heat stress and a control
373 arm which was not exposed to heat stress (Figure 1A and B) to compensate for these effects.

374 To begin the experiment, a single culture of Philadelphia-1 was divided into 12 independent lineages to
375 assess the parallelism between adaptive paths, divided into six evolved lineages that were exposed to
376 heat shock and six control lineages that were not. Each population was grown in AYE overnight to

377 stationary phase. Bacteria were triply washed in Fraquil, suspended at OD_{600} 0.1 (approximately 10^8
378 CFU/mL) and incubated for 24 hours at room temperature, as in (98). For each suspension, 1 mL was
379 dispensed into a 13 mL polypropylene culture tube (Sarstedt). Tubes of the treated lineage were
380 immersed for 15 minutes in a pre-heated water bath set to the challenge temperature (55°C to 59°C).
381 Samples were withdrawn from the water bath and cooled passively to room temperature. Tubes of the
382 control lineages were left at room temperature. Control lineages were propagated by inoculating 1.5 mL
383 AYE with 15 µL (approximately 1.5 x 10^6 CFU) of the untreated suspension, to mimic the population
384 bottleneck created by heat shock. Evolved lineages were propagated by inoculating 750 µL of 2x
385 concentrated AYE with 750 µL of the heat-treated suspension. Cultures were grown overnight to
386 stationary phase, as before, and a 100 µL aliquot was stored at -80 °C in AYE + 15% glycerol to maintain a
387 frozen archive of the full population at each passage.

388 The experiment was continued for 70 passages with the temperature of heat stress increased on an *ad-*
389 *hoc* basis to maintain the strength of selective pressure. Based on preliminary experiments, the
390 experiment was begun with a 15-minute exposure to 55 °C. After 10 passages under selection, this was
391 increased to 57 °C. This was further increased to 58 °C after 30 passages and finally to 59 °C after 50
392 passages.

393 Heat shock survival measurements

394 Following the conclusion of the experiment, heat adapted populations were resuscitated from frozen
395 stocks, grown on CYE, and suspended in Fraquil as above. All lineages were tested at five passage intervals
396 for heat shock survival after 20 minutes of exposure to 55 °C, 57 °C, and 59 °C in 60 µL volumes
397 simultaneously in a Veriti 96-well thermocycler and actively cooled to 20 °C, with control samples held at
398 room temperature. CFU counts were determined by serial dilution and plating in 10 µL aliquots on CYE
399 plates.

400 A similar strategy was used to determine the heat shock tolerance of mutants expressing the various
401 derived alleles of *htpG*. Samples were prepared and aliquoted as above and exposed to 55 °C for 0, 10,
402 20, and 30 minutes in a Veriti 96-well thermocycler and actively cooled to 20 °C. CFU counts were
403 conducted as above and normalized to the CFU count of the 0 minutes exposure sample.

404 Isolate collection and sequencing strategy

405 Single colonies were isolated from the populations generated after 70 passages and stored at -80 °C. Ten
406 isolates were collected from each heat-adapted lineage and five isolates were collected from each control
407 lineage. In addition, we resequenced our lab stock of Philadelphia-1 to identify any mutations that were
408 fixed in the ancestral population at the outset of the ALE. DNA was collected from these isolates using the
409 Wizard Genomic DNA Purification kit (Promega) and submitted to the McGill Genome Center for library
410 preparation and sequencing using a 600 cycle MiSeq v3 reagent kit.

411 Fastp (99) with default settings was used to both clean and perform quality control on paired-end reads.
412 Read alignment and variant calling were conducted using Breseq 0.35.4 (100), bowtie2 2.3.5.1 (101, 102),
413 and R 4.0.3 (103) with the NCBI-deposited sequence (CP015927.1) of the ancestral Philadelphia-1 ATCC
414 33152 strain as reference genome. Because the per-isolate read coverage was low (mean = 14.37, s =
415 2.37), there were often regions of missing coverage lacking aligned reads to confidently assign allele
416 identity. To increase the depth of coverage, we analyzed pooled per-lineage sequence data by combining
417 the reads together of all ten sampled isolates for each heat-adapted lineage or all five sampled isolates
418 for each control lineage to reconstruct the allele frequencies in the final populations. We re-analyzed
419 these pooled reads using Breseq using the same parameters to generate our final list of called variants.

420 qPCR protocol and analysis

421 RNA was collected from 1 ml samples of *L. pneumophila* suspended at an OD_{600} of 1 either heat shocked
422 at 55 °C for 15 minutes or held at room temperature for the same duration using TRIzol (ThermoFisher

423 Scientific), as previously described. RNA samples were treated with DNase I and Dnase inactivation
424 reagent (ThermoFisher Scientific) before quantification and storage in nuclease-free water (ThermoFisher
425 Scientific) at -20 °C until required. Protoscript II (New England Biolabs) was used to reverse transcribe RNA
426 into cDNA as template for qPCR analysis using the manufacturer's protocol. No-RT control reactions were
427 produced in the same way with nuclease-free water replacing Protoscript II.

428 All qPCR experiments were performed in an Applied Biosystems 7500 Fast Real-Time PCR machine using
429 iTaq Universal SYBR-green supermix (BioRad). Efficiencies for qPCR primers (Table 2) were calculated using
430 a serial dilution of gDNA samples, and all were found to be acceptable (90.9 - 96.8%) (104). 16S rRNA was
431 used as a common housekeeping gene to normalize Ct values (75) and efficiency-adjusted ddCT (105) was
432 used to compare RNA expression levels between bacteria exposed and naive to heat shock.

433 Mutant construction

434 To determine the role of HtpG over the ALE procedure, we constructed merodiploids by supplementing
435 the various derived alleles of *htpG* on a plasmid. Plasmids were constructed on a pXDC39 backbone
436 allowing *htpG* to be expressed under its native promoter. Using Phusion polymerase and primers kpni-
437 htpg-F and xbai-htpg-R, we amplified the treated lineages T3 ($htpG^{G83E}$), T5 ($htpG^{Q148*}$), and T6 ($htpG^{\Delta 1bp}$
438 ^{503nt}) alleles from the purified gDNA of single isolates from passage 70. These fragments, carrying the gene
439 sequence and its upstream region, were ligated into pXDC39 to produce plasmids p$htpG^{G83E}$, p$htpG^{Q148*}$,
440 and p$htpG^{\Delta 1bp\ 503nt}$. These plasmids were electroporated into a previously constructed KS79-based *htpG*
441 deletion mutant (75) to assay for relative fitness and to isolate the derived *htpG* alleles onto a wild-type
442 background.

443 Direct fitness competition in AYE

444 To determine the relative competitive fitness of *L. pneumophila* before and after our ALE model, we
445 constructed strains that could be co-cultured in AYE and distinguished by the presence or absence of GFP.

446 The GFP-negative control vector pMMB207c and the GFP-positive pXDC31 are distinguished by the
447 insertion of an GFP coding sequence whose expression is driven by pTac and ultimately induced by IPTG.
448 Both plasmids were introduced into the wild-type ancestor Philadelphia-1 and the derived lineages C-1
449 and HA-1 by electroporation, as previously described (75). A single isolate was collected from each
450 electroporation to represent the fitness of the population in competition.
451 Strain pairs containing these two plasmids were separately grown overnight and normalized to an OD_{600}
452 of 0.1 in AYE supplemented with chloramphenicol for use in a direct competition assay, described in brief
453 below. Competitions were carried out under standard incubation conditions. For each replicate, 500 µL of
454 each culture of the strain pair were combined at a 1:1 ratio. A 100 µL sample of this mixture was used to
455 inoculate 900 µL AYE with chloramphenicol and adjusted to a final OD_{600} of 0.01 and incubated overnight.
456 The overnight culture was diluted to an OD600 of 0.01 and used to continue the assay in the same way
457 for a total of three transfers. CFU concentration for each timepoint was counted by serial dilution plating
458 on AYE with chloramphenicol and IPTG. Population fractions were manually counted under a UV black
459 light to distinguish between fluorescent and non-fluorescent colonies.

460 ## Host cell infection

461 *Vermamoeba vermiformis* was used as a permissive host to assess the infectivity of *L. pneumophila*. The
462 amoeba was routinely grown in 25 mL vented flasks (Sarstedt, Corning) at room temperature and
463 passaged twice a week in modified PYNFH media with FBS and buffer. Amoeba populations were
464 expanded in 75 mL flasks 3 days before infection and harvested by centrifugation at 200 × *g* for 10 minutes.

465 Host cells were normalized in modified PYNFH without FBS or buffer at 5 x 10^5 cells/ml and 1 mL was
466 added to each well of a 24-well cell culture plate. Infectious bacteria were collected from fresh colonies
467 on CYE plates and normalized in Fraquil to an OD of OD_{600} 0.01 (approximately 10^7 CFU/mL). To start
468 infections with an MOI of 0.1, 5 µL bacterial suspension was added to each well and the initial CFU count

469 was conducted on the gently mixed supernatant. Growth was carried out for 3 days at 37 °C with CFU
470 counts performed daily.

471 Western blotting

472 Protein samples for Western blotting were prepared using a modified version of the Bio-Rad
473 electrophoresis guide (42). Briefly, *L. pneumophila* pellets were harvested by centrifugation from a 200 µl
474 sample of overnight culture rinsed in Fraquil and normalized to an OD_{600} of 1. Pellets were homogenized
475 by bath sonication (Cole-Parmer) on ice for 10 minutes after thorough suspension in 200 µl sample
476 solubilization buffer. Samples were diluted with 250 µl 2X Laemmli sample buffer (BioRad) and held at
477 room temperature for 20 minutes. The sample was centrifuged for 30 minutes, and the protein sample
478 was collected from the resulting supernatant.

479 The proteins were migrated in hand-cast 12.5% polyacrylamide gels (BioRad) at 50 V for 30 minutes and
480 120 V for 90 minutes. Separated proteins were transferred onto polyvinylidene difluoride (OVDF)
481 membranes (BioRad) at 25 V for 12 hours at 4 °C in preparation for immunoblotting and blocked using
482 TBS wash buffer with 5% skim milk powder. Ab225994 (rabbit anti-*E. coli* HtpG; AbCam) was found to be
483 cross-reactive to *L. pneumophila* HtpG and was used as the primary antibody at a 1:5000 dilution, along
484 with rabbit anti-IcdH (Sigma-Aldrich) (1:10000) as a loading control. Primary incubation was carried out
485 for 2 hours, followed by rinsing and blotting with a 1:5000 goat anti-rabbit HRP (Sigma-Aldrich) for 1 hour.
486 Bands were developed using a ECL Prime Western Blotting Detection Reagent (Cytiva BioSciences) and
487 imaged using a ChemiDoc MP Imaging System.

488 Data Availability

489 Raw read data from sequenced isolates collected after 30 and 70 passages have been deposited to the
490 National Center for Biotechnology Availability's sequence read archive and are available under BioProject
491 Accession number PRJNA956983.

Acknowledgements

Many thanks to Jesse Shapiro for providing guidance on ALE. This work was supported by a Natural Science and Engineering Research Council of Canada Discovery Grant (RGPIN/04499-2018) to SPF. JL was the recipient of a Canada Graduate Scholarship—Master's award from the Natural Science and Engineering Research Council of Canada.

497 # Figures

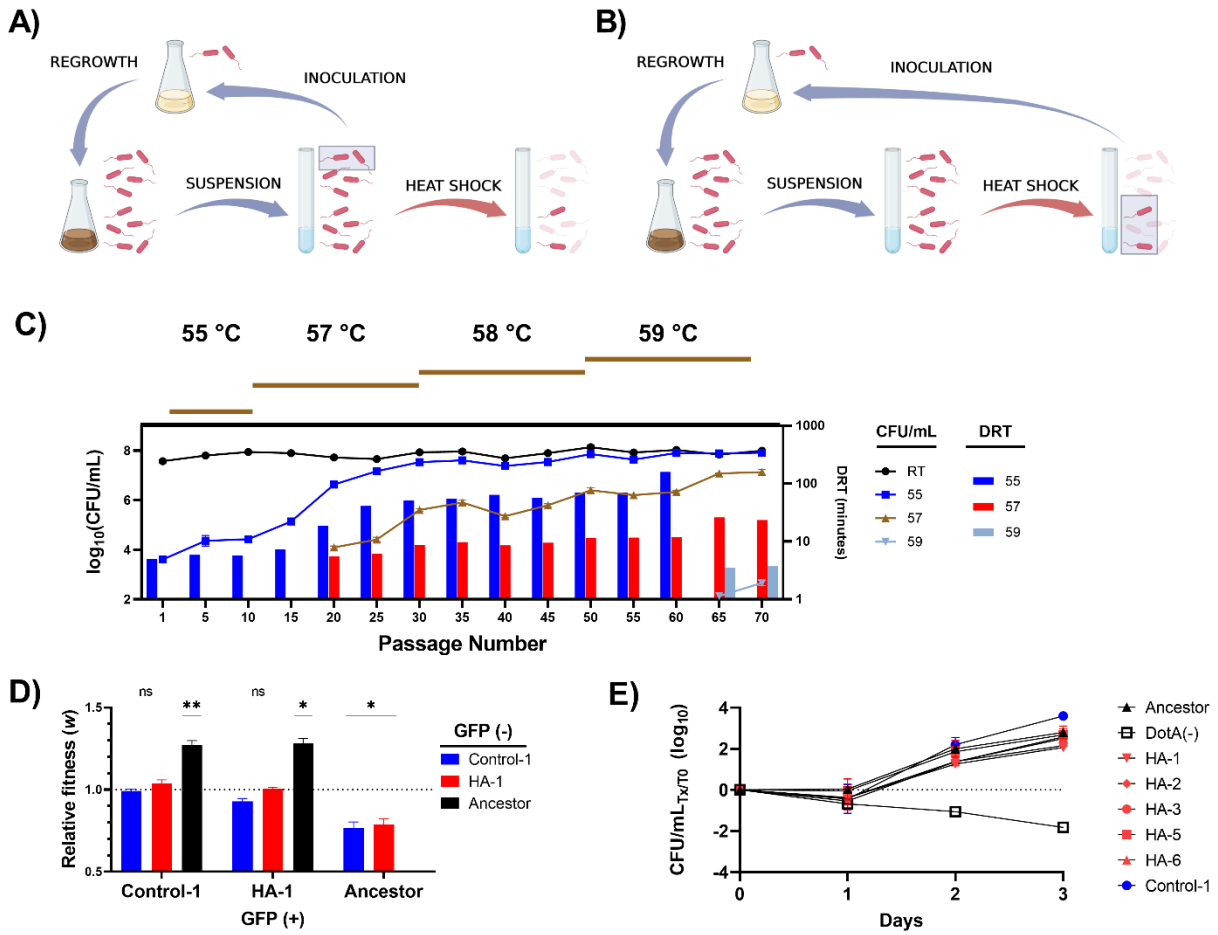

498

499 **Figure 1. ALE increased the resistance of *L. pneumophila* to heat shock.** The organization of the ALE
500 protocol, contrasting the heat-adaptation (A) and control (B) branches (Created with BioRender). Each
501 panel depicts one of 70 cycles, with highlighted rectangles showing the population bottleneck for each
502 branch. In brief, after collection from post-exponential growth in AYE and 24-hour suspension in Fraquil,
503 control lineages were propagated by subsampling the suspended population to re-inoculate AYE while
504 heat-adapted lineages were propagated by re-inoculating AYE with the population surviving heat shock.
505 C) Survival of heat-adapted *L. pneumophila* lineages following 20 minutes of exposure to 55, 57, and 59
506 °C heat shock for 20 minutes (lines, left axis). Decimal reduction times (DRT) were calculated for each

507 temperature and are plotted for each tested passage (right axis, bar; omitted for passages 65 and 70 at
508 55 °C because there was an insignificant level of cell death). D) Direct competition between green-
509 fluorescent isolates and non-fluorescent isolates growing in AYE. Significance calculations show one-
510 sample *t*-test against 1.0 (neutral relative fitness), $n = 3$. E) Infection and replication within *V. vermiformis*
511 in modified PYNFH without FBS, $n = 3$. The avirulent DotA(-) strain is used as a negative control.

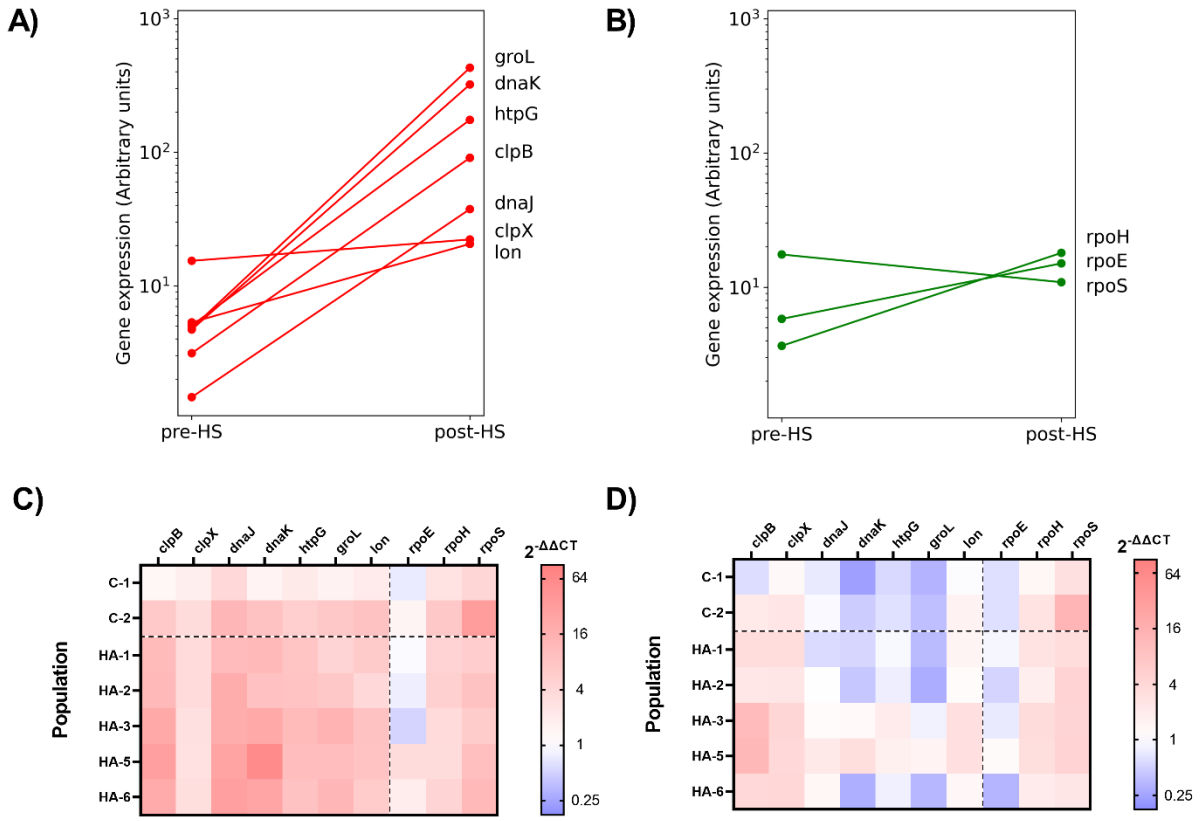

Figure 2: qPCR analysis of RNA expression levels in the ancestor Philadelphia-1 following 5 minutes of exposure to 55 °C heat shock for heat-shock response genes (A) and sigma factors (B). Ct values were normalized using 16S rRNA levels and converted to arbitrary expression levels, $n = 3$. Relative difference in expression in RNA samples collected before heat shock (C) and after heat shock (D) between sampled populations (C, control lineages; HA, heat-adapted lineages) and Philadelphia-1, $n = 3$.

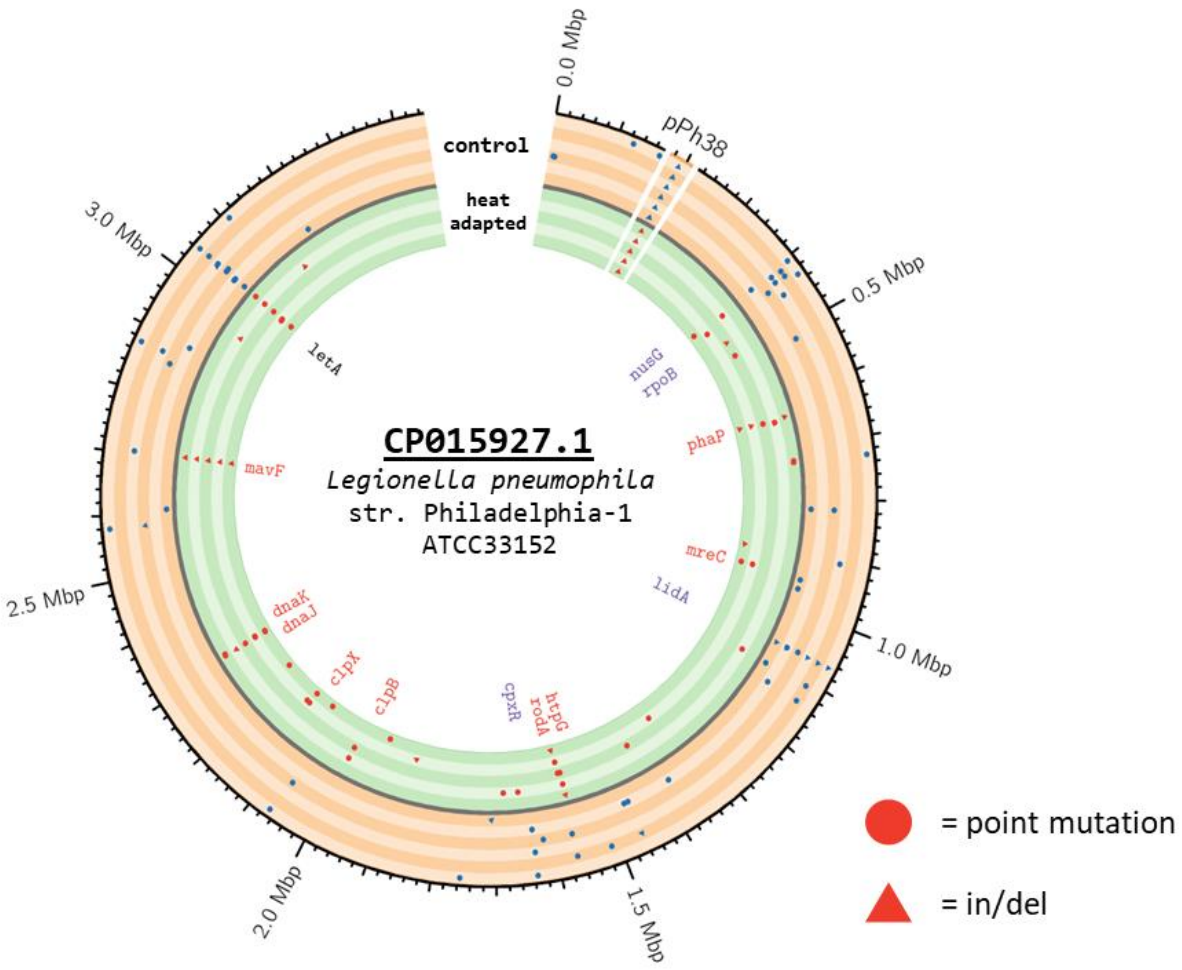

Figure 3: Derived mutations identified with Breseq at a frequency of at least 25% in replicate control and heat-adapted lineages aligned to the genome of the ancestral strain Philadelphia-1 (106). The outermost concentric circle shows the single chromosome of *L. pneumophila*, as well as a reversibly-integrated pPh38 element which was not retained in our lab strain. Each band shows the mutations observed across control lineage (orange) and heat-adapted (green), with circles representing point mutations and triangles representing insertions and deletions. Genes of interest in the interior are labelled by colour with red genes mutated in multiple heat-adapted lineages and blue genes mutated in multiple control lineages.

526

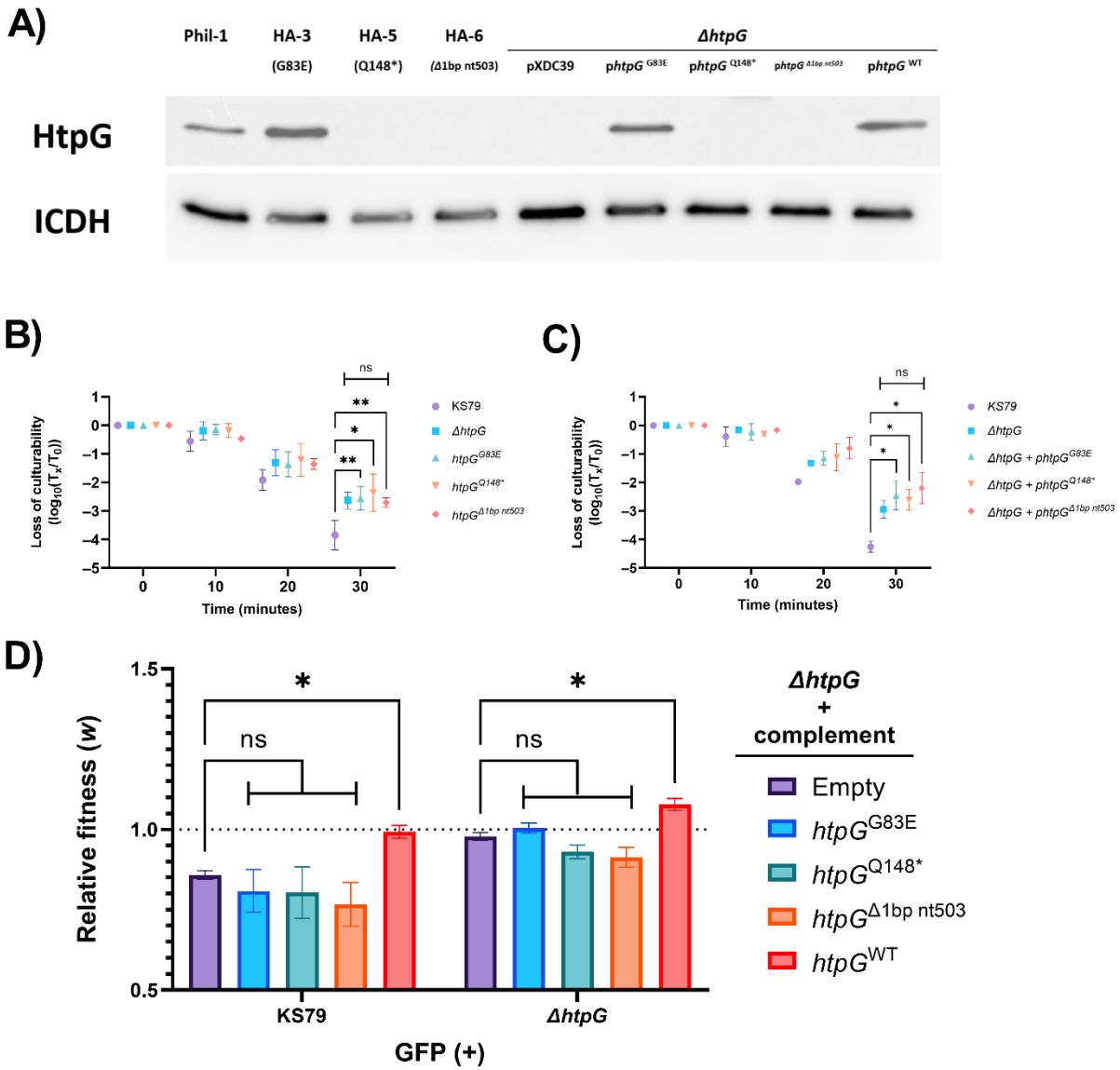

527

528 **Figure 4:** A) Anti-*htpG* Western blots visualizing the expression of HtpG in lineages HA-3, 5 and 6 and in

529 constructed merodiploid mutants. B) Survival at 55 °C of knock-in exchange mutants expressing derived

530 alleles of *htpG* in place of the wild-type allele, $n = 3$. C) Survival at 55 °C of an *htpG* deletion mutant

531 heterologously expressing different alleles of *htpG* found in treated lineages, $n = 3$. D) Relative fitness of

532 the *htpG* deletion mutant complemented with an empty plasmid, derived, or ancestral *htpG* against the

533 wild-type and deletion mutant strains.

534 # Tables

535 Table 1: Bacterial strains and plasmids used in this study. Except where noted, all strains used were of *L.*
536 *pneumophila*

Strain	Description	Source
Philadelphia-1	Philadelphia 1976	ATCC33152
KS79	JR32 ΔcomR	(107)
Δ*htpG*	KS79 *htpG*::Kn^{pSF6}	(75)
htpG^{G83E}	KS79 *htpG*::*htpG*$^{HA-3}$ + *Kn* $^{pGEMT-easy}$	This study
htpG^{Q148*}	KS79 *htpG*::*htpG*$^{HA-5}$ + *Kn* $^{pGEMT-easy}$	This study
htpG$^{\Delta 1bp\ nt603}$	KS79 *htpG*::*htpG*$^{HA-6}$ + *Kn* $^{pGEMT-easy}$	This study
E. coli DH5α	supE44 ΔlacU169 (Φ80lacZΔM15) hsdR17 recA1 endA1 gyrA96 thi-1 relA1	Invitrogen
Plasmid	**Description**	**Source**
pMMB207c	RSF1010 derivative, IncQ, lacIq, Cm^r, Ptac, oriT, ΔmobA	(108)
pXDC39	pMMB207c ΔPtac, ΔlacI, Cmr	Xavier Charpentier
pSF6	pGEMT-easy-rrnb	(109)
pXDC31	pMMB207C + *gfp*	(110)
p*htpG*^{G83E}	pXDC39 + *htpG*$^{HA-3}$	This study
p*htpG*^{Q148*}	pXDC39 + *htpG*$^{HA-5}$	This study
p*htpG*$^{\Delta 1bp\ nt603}$	pXDC39 + *htpG*$^{HA-6}$	This study
p*htpG*^{WT}	pXDC39 + *htpG*$^{Philadelphia-1}$	(75)

537

538 Table 2: All primers used during this study

Primer	Sequence 5'-3	Source
Primers for qPCR		
groL-qPCR-F	GAACATGGGCGCTCAAATGG	This study
groL-qPCR-R	GCAGCAACTGCTTTGTGACC	This study
lon-qPCR-F	GTTGCTTCAGCAGACATCGG	This study
lon-qPCR-R	GCTGGAATGCCGAAAGAAGC	This study
rpoH-qPCR-F	CCCATCTTGGGGTCAAAACG	This study
rpoH-qPCR-R	CGCGGTTATCTGGGGTATGG	This study
rpoE-qPCR-F	CCAGGTTGAAAACTGACTGCG	This study
rpoE-qPCR-R	CTGTTTGAGCGTTATCAGGGC	This study
rpoS-qPCR-F	ATGCGACCTGGTGGATTAGG	This study
rpoS-qPCR-R	TTTGCGTCAATTGCCTTGCC	This study
phaP-qPCR-F	CTGAACTGAATGTTAAAACCCTGC	This study
phaP-qPCR-R	TTTTCCAGCATTTCTTCGGGC	This study
htpg-qPCR-F	TTACATACCAGCCCATGCCC	This study
htpg-qPCR-R	TCGGGGTAAAAATTGTGTCGC	This study
clpb-qPCR-F	CACTTGCAGATGCCCAATCC	This study
clpb-qPCR-R	AGAGGTCTGCAACTTCCACC	This study
clpx-qPCR-F	ATTAAGAATCCGCGCCAGGG	This study
clpx-qPCR-R	GAGGATGGTGTTGAGCTCGG	This study
dnaj-qPCR-F	TTTGTCCACGTGATTGACGC	This study
dnaj-qPCR-R	ATCCTTCAATGGGTGGAGGC	This study
dnak-qPCR-F	CGCAATAACAGAGTCACCGC	This study
dnak-qPCR-R	GCAACCAAAGATGCTGGTCG	This study
16s-qPCR-F	AGAGATGCATTAGTGCCTTCGGGA	(75)
16s-qPCR-R	ACTAAGGATAAGGGTTGCGCTCGT	(75)
Primers for mutant construction		
htpG-UF	CTTGCACATCTTGGAAAAGGAGG	(75)
htpG-UR	CAGTCTAGCTATCGCCATGTACTCCCCGTTAATAGTTGTGTTCG	(75)
htpG-KnF	CGAACACAACTATTAACGGGGAGTACATGGCGATAGCTAGACTG	(75)
htpG-KnR	GCTCATCCCGGATAATGACTTGTACCCAACTGATCTTCAGCATC	(75)

htpG-DF	GATGCTGAAGATCAGTTGGGTACAAGTCATTATCCGGGATGAGC	(75)
htpG-DR	CAATTATTGCCTTACTGCCTGGG	(75)
Primers for complementation		
KpnI-HtpG-F	TCATCAGGTACCTGAATCGAGAGGGTTTGAGTTGG	(75)
XbaI-HtpG-R	TCATCATCTAGAGGATAATGACTTGTTGTAATCCGGG	(75)

539

540

541 Table 3: Selected mutations derived over the course of the ALE determined from Breseq analysis of
542 pooled Illumina short reads. The table includes non-synonymous mutations which emerged in two or
543 more lineages of either the control or heat-adapted protocol branches. All mutations listed were
544 present in at least 25% of pooled sequence reads.

	C-1	C-2	C-3	C-4	C-5	C-6	HA-1	HA-2	HA-3	HA-5	HA-6
pPh38	Δ37,890 bp chr1: 173323	Δ37,890 bp chr1: 173323	Δ37,890 bp chr1: 173323	Δ37,890 bp chr1: 173323	Δ37,890 bp chr1: 173323	Δ37,890 bp chr1: 173323	Δ37,890 bp chr1: 173323	Δ37,890 bp chr1: 173323	Δ37,890 bp chr1: 173323	Δ37,890 bp chr1: 173323	Δ37,890 bp chr1: 173323
two-component system response regulator LetA	L68R	L68R	L68R	L68R	L68R	L68R	L68R	L68R	L68R	L68R	L68R
transcription termination/antitermination protein NusG		R136I				V143D					
DNA-directed RNA polymerase subunit beta				G759E	N1350T		G138E			K924N	
30S ribosomal protein S10				Q36K	S102N						
hypothetical protein (phasin)							Δ1bp nt39	Δ1bp nt39			+A 38
rod shape-determining protein MreC							V266A	V266A			
LidA	Δ1bp nt1566	Δ1bp nt1122, P330R	E508*	Δ1bp nt1566	Δ1bp nt1122	Δ1bp nt1566					
molecular chaperone HtpG									G83E	Q148*	Δ1bp nt503
rod shape-determining protein RodA			A128T		A128T			R112S	P332S		
transcriptional regulatory protein CpxR		R112L		D190N		D194N					
ATP-dependent chaperone ClpB									A478V	A492T	
ATP-dependent protease ATP-binding subunit ClpX							G202A	E203D			
molecular chaperone DnaJ							F95Y	F95Y	P334S	+C 1100	R318T

molecular chaperone DnaK							M94I	V373L, M94I			M94I
hypothetical protein (mavF)							Δ1bp nt368	Δ1bp nt368	Δ1bp nt368	Δ1bp nt368	+T 456
NADH-quinone oxidoreductase subunit G										G455D	E768K

545

546

547 # References

548 1. Al-Quadan T, Price CT, Abu Kwaik Y. 2012. Exploitation of evolutionarily conserved amoeba and
549 mammalian processes by Legionella. Trends Microbiol 20:299–306.

550 2. Cunha BA, Burillo A, Bouza E. 2016. Legionnaires' disease, p. 376–385. *In* The Lancet. Lancet
551 Publishing Group.

552 3. Springston JP, Yocavitch L. 2017. Existence and control of Legionella bacteria in building water
553 systems: A review. J Occup Environ Hyg 14:124–134.

554 4. Greco SL, Drudge C, Fernandes R, Kim JH, Copes R. 2020. Estimates of Healthcare Utilization and
555 Deaths from Waterborne Pathogen Exposure in Ontario, Canada. Epidemiol Infect 148:1–10.

556 5. Kool JL, Fiore AE, Kioski CM, Brown EW, Benson RF, Pruckler JM, Glasby C, Butler JC, Cage GD,
557 Carpenter JC, Mandel RM, England B, Breiman RF. 1998. More than 10 Years of Unrecognized
558 Nosocomial Transmission of Legionnaires' Disease among Transplant Patients. Infect Control
559 Hosp Epidemiol 19:898–904.

560 6. Phin N, Parry-Ford F, Harrison T, Stagg HR, Zhang N, Kumar K, Lortholary O, Zumla A, Abubakar I.
561 2014. Epidemiology and clinical management of Legionnaires' disease. Lancet Infect Dis 14:1011–
562 1021.

563 7. Fraser DW, Tsai TR, Orenstein W, Parkin WE, Beecham HJ, Sharrar RG, Harris J, Mallison GF,
564 Martin SM, McDade JE, Shepard CC, Brachman PS, Fraser, David W. and Tsai, Theodore R. and
565 Orenstein, Walter and Parkin, William E. and Beecham, H. James and Sharrar, Robert G. and
566 Harris, John and Mallison, George F. and Martin, Stanley M. and McDade, Joseph E. and Shepard,
567 Charles C. and Brachman PS, Fraser DW, Tsai TR, Orenstein W, Parkin WE, Beecham HJ, Sharrar

568 RG, Harris J, Mallison GF, Martin SM, McDade JE, Shepard CC, Brachman PS. 1977. Legionnaires'
569 disease: description of an epidemic of pneumonia. N Engl J Med 297:1189–11897.

570 8. Tobin JO, Bartlett CL, Waitkins SA, Barrow GI, Macrae AD, Taylor AG, Fallon RJ, Lynch FR. 1981.
571 Legionnaires' disease: Further evidence to implicate water storage and distribution systems as
572 sources. Br Med J 282:573.

573 9. Prussin AJ, Schwake DO, Marr LC. 2017. Ten questions concerning the aerosolization and
574 transmission of Legionella in the built environment. Build Environ 123:684–695.

575 10. Boppe I, Bédard E, Taillandier C, Lecellier D, Nantel-Gauvin MA, Villion M, Laferrière C, Prévost M.
576 2016. Investigative approach to improve hot water system hydraulics through temperature
577 monitoring to reduce building environmental quality hazard associated to Legionella. Build
578 Environ 108:230–239.

579 11. Colbourne JS, Pratt DJ, Smith MG, Fisher-Hoch SP, Harper D. 1984. Water Fittings as Sources of
580 Legionella pneumophila in a Hospital Plumbing System. The Lancet 323:210–213.

581 12. David S, Mentasti M, Lai S, Vaghji L, Ready D, Chalker VJ, Parkhill J. 2018. Spatial structuring of a
582 legionella pneumophila population within the water system of a large occupational building.
583 Microb Genomics 4.

584 13. Van Kenhove E, Dinne K, Janssens A, Laverge J. 2019. Overview and comparison of Legionella
585 regulations worldwide. Am J Infect Control 47:968–978.

586 14. Declerck P. 2010. Biofilms: The environmental playground of Legionella pneumophila. Environ
587 Microbiol 12:557–566.

588 15. Farhat M, Moletta-Denat M, Frère J, Onillon S, Trouilhé MC, Robine E. 2012. Effects of
589 disinfection on legionella spp., eukarya, and biofilms in a hot water system. Appl Environ
590 Microbiol 78:6850–6858.

591 16. Bédard E, Lévesque S, Martin P, Pinsonneault L, Paranjape K, Lalancette C, Dolcé CÉ, Villion M,
592 Valiquette L, Faucher SP, Prévost M. 2016. Energy Conservation and the Promotion of Legionella
593 pneumophila Growth: The Probable Role of Heat Exchangers in a Nosocomial Outbreak. Infect
594 Control Hosp Epidemiol 37:1475–1480.

595 17. Peiró Callizo EF, Sierra JD, Pombo JMS, Baquedano CE, Huerta BP. 2005. Evaluation of the
596 effectiveness of the Pastormaster method for disinfection of legionella in a hospital water
597 distribution system. J Hosp Infect 60:150–158.

598 18. Almeida D, Cristovam E, Caldeira D, Ferreira JJ, Marques T. 2016. Are there effective
599 interventions to prevent hospital-acquired Legionnaires' disease or to reduce environmental
600 reservoirs of Legionella in hospitals? A systematic review. Am J Infect Control 44:e183–e188.

601 19. USEPA. 2016. Technologies for Legionella Control in Premise Plumbing Systems: Scientific
602 Literature ReviewEPA, Office of Water. United States Environmental Protection Agency.

603 20. Vervaeren H, Temmerman R, Devos L, Boon N, Verstraete W. 2006. Introduction of a boost of
604 Legionella pneumophila into a stagnant-water model by heat treatment. FEMS Microbiol Ecol
605 58:583–592.

606 21. Lin YE, Stout JE, Yu VL. 2011. Controlling Legionella in Hospital Drinking Water: An Evidence-
607 Based Review of Disinfection Methods. Infect Control Hosp Epidemiol 32:166–173.

608 22. Whiley H, Bentham R, Brown MH. 2017. Legionella persistence in manufactured water systems:
609 Pasteurization potentially selecting for thermal tolerance. Front Microbiol 8.

610 23. Allegra S, Grattard F, Girardot F, Riffard S, Pozzetto B, Berthelot P. 2011. Longitudinal evaluation
611 of the efficacy of heat treatment procedures against Legionella spp. in hospital water systems by
612 using a flow cytometric assay. Appl Environ Microbiol 77:1268–1275.

613 24. Bédard E, Boppe I, Kouamé S, Martin P, Pinsonneault L, Valiquette L, Racine J, Prévost M. 2016.
614 Combination of heat shock and enhanced thermal regime to control the growth of a persistent
615 Legionella pneumophila strain. Pathogens 5:1–3.

616 25. Steinert M, Ockert G, Lück C, Hacker J. 1998. Regrowth of Legionella pneumophila in a heat-
617 disinfected plumbing system. Zentralblatt Bakteriol 288:331–342.

618 26. Kramer B, Thielmann J. 2016. Monitoring the live to dead transition of bacteria during thermal
619 stress by a multi-method approach. J Microbiol Methods 123:24–30.

620 27. Mitsuzawa S, Deguchi S, Horikoshi K. 2006. Cell structure degradation in Escherichia coli and
621 Thermococcus sp. strain Tc-1-95 associated with thermal death resulting from brief heat
622 treatment. FEMS Microbiol Lett 260:100–105.

623 28. Richter K, Haslbeck M, Buchner J. 2010. The Heat Shock Response: Life on the Verge of Death.
624 Mol Cell 40:253–266.

625 29. Binder SC, Eckweiler D, Schulz S, Bielecka A, Nicolai T, Franke R, Häussler S, Meyer-Hermann M.
626 2016. Functional modules of sigma factor regulons guarantee adaptability and evolvability. Sci
627 Rep 6:22212.

628 30. Nonaka G, Blankschien M, Herman C, Gross CA, Rhodius VA. 2006. Regulon and promoter analysis
629 of the E. coli heat-shock factor, σ32, reveals a multifaceted cellular response to heat stress.
630 Genes Dev 20:1776–1789.

631 31. Basta DW, Angeles-Albores D, Spero MA, Ciemniecki JA, Newman DK. 2020. Heat-shock proteases
632 promote survival of Pseudomonas aeruginosa during growth arrest. Proc Natl Acad Sci U S A
633 117:4358–4367.

634 32. Feder ME, Hofmann GE. 1999. Heat-shock proteins, molecular chaperones, and the stress
635 response: Evolutionary and ecological physiology. Annu Rev Physiol 61:243–282.

636 33. McCarty JS, R üdiger S, Sch önfeld H-J, Schneider-Mergener J, Nakahigashi K, Yura T, Bukau B.
637 1996. Regulatory Region C of the E. coli Heat Shock Transcription Factor, σ32, Constitutes a DnaK
638 Binding Site and is Conserved Among Eubacteria. J Mol Biol 256:829–837.

639 34. Yura T. 2019. Regulation of the heat shock response in Escherichia coli: History and perspectives.
640 Genes Genet Syst 94:103–108.

641 35. Lema MW, Brown A, Butler CA, Hoffman PS. 1988. Heat-shock response in Legionella
642 pneumophila. Can J Microbiol 34:1148–1153.

643 36. Cazalet C, Rusniok C, Brüggemann H, Zidane N, Magnier A, Ma L, Tichit M, Jarraud S, Bouchier C,
644 Vandenesch F, Kunst F, Etienne J, Glaser P, Buchrieser C. 2004. Evidence in the Legionella
645 pneumophila genome for exploitation of host cell functions and high genome plasticity. Nat
646 Genet 36:1165–1173.

647 37. Chien M, Morozova I, Shi S, Sheng H, Chen J, Gomez SM, Asamani G, Hill K, Nuara J, Feder M,
648 Rineer J, Greenberg JJ, Steshenko V, Park SH, Zhao B, Teplitskaya E, Edwards JR, Pampou S,

649 Georghiou A, Chou I-C, Iannuccilli W, Ulz ME, Kim DH, Geringer-Sameth A, Goldsberry C, Morozov
650 P, Fischer SG, Segal G, Qu X, Rzhetsky A, Zhang P, Cayanis E, De Jong PJ, Ju J, Kalachikov S,
651 Shuman HA, Russo JJ. 2004. The genomic sequence of the accidental pathogen Legionella
652 pneumophila. Science 305:1966–1968.

653 38. Garduño RA, Chong A, Nasrallah GK, Allan DS. 2011. The Legionella pneumophila chaperonin - An
654 unusual multifunctional protein in unusual locations. Front Microbiol 2:122.

655 39. Li XH, Zeng YL, Gao Y, Zheng XC, Zhang QF, Zhou SN, Lu YJ. 2010. The ClpP protease homologue is
656 required for the transmission traits and cell division of the pathogen Legionella pneumophila.
657 BMC Microbiol 10:54.

658 40. Zhao BB, Li XH, Zeng YL, Lu YJ. 2016. ClpP-deletion impairs the virulence of Legionella
659 pneumophila and the optimal translocation of effector proteins. BMC Microbiol 16:1–12.

660 41. Mendis N, McBride P, Saoud J, Mani T, Faucher SP. 2018. The LetA/S two-component system
661 regulates transcriptomic changes that are essential for the culturability of Legionella
662 pneumophila in water. Sci Rep 8:6764.

663 42. Saoud J, Mani T, Faucher SP. 2021. The Tail-Specific Protease Is Important for Legionella
664 pneumophila To Survive Thermal Stress in Water and inside Amoebae. Appl Environ Microbiol
665 87:1–15.

666 43. Barrick JE, Lenski RE. 2013. Genome dynamics during experimental evolution. Nat Rev Genet
667 14:827–839.

668 44. Bruger EL, Marx CJ. 2018. A decade of genome sequencing has revolutionized studies of
669 experimental evolution. Curr Opin Microbiol 45:149–155.

670 45. Dykhuizen D. 2016. Thoughts toward a theory of natural selection: The importance of microbial
671 experimental evolution. Cold Spring Harb Perspect Biol 8:a018044.

672 46. Frenkel EM, McDonald MJ, Van Dyken JD, Kosheleva K, Lang GI, Desai MM. 2015. Crowded
673 growth leads to the spontaneous evolution of semistable coexistence in laboratory yeast
674 populations. Proc Natl Acad Sci U S A 112:11306–11311.

675 47. Bruckbauer ST, Trimarco JD, Martin J, Bushnell B, Senn KA, Schackwitz W, Lipzen A, Blow M,
676 Wood EA, Culberson WS, Pennacchio C, Cox MM. 2019. Experimental evolution of extreme
677 resistance to ionizing radiation in Escherichia coli after 50 cycles of selection. J Bacteriol 201.

678 48. Deatherage DE, Kepner JL, Bennett AF, Lenski RE, Barrick JE. 2017. Specificity of genome
679 evolution in experimental populations of Escherichia coli evolved at different temperatures. Proc
680 Natl Acad Sci U S A 114:E1904–E1912.

681 49. Harden MM, He A, Creamer K, Clark MW, Hamdallah I, Martinez KA, Kresslein RL, Bush SP,
682 Slonczewski JL. 2015. Acid-Adapted Strains of Escherichia coli K-12 Obtained by Experimental
683 Evolution. Appl Environ Microbiol 81:1932–1941.

684 50. Almahmoud I, Kay E, Schneider D, Maurin M. 2009. Mutational paths towards increased
685 fluoroquinolone resistance in Legionella pneumophila. J Antimicrob Chemother 64:284–293.

686 51. Descours G, Ginevra C, Jacotin N, Forey F, Chastang J, Kay E, Etienne J, Lina G, Doublet P, Jarraud
687 S. 2017. Ribosomal Mutations Conferring Macrolide Resistance in Legionella pneumophila.
688 Antimicrob Agents Chemother 61:e02188-16.

689 52. Ensminger AW, Yassin Y, Miron A, Isberg RR. 2012. Experimental evolution of Legionella
690 pneumophila in mouse macrophages leads to strains with altered determinants of environmental
691 survival. PLoS Pathog 8:e1002731.

692 53. Cervero-Aragó S, Schrammel B, Dietersdorfer E, Sommer R, Lück C, Walochnik J, Kirschner A.
693 2019. Viability and infectivity of viable but nonculturable Legionella pneumophila strains induced
694 at high temperatures. Water Res 158:268–279.

695 54. Rhoads WJ, Ji P, Pruden A, Edwards MA. 2015. Water heater temperature set point and water use
696 patterns influence Legionella pneumophila and associated microorganisms at the tap.
697 Microbiome 3:67.

698 55. Burmann BM, Schweimer K, Luo X, Wahl MC, Stitt BL, Gottesman ME, Rösch P. 2010. A
699 NusE:NusG Complex Links Transcription and Translation. Science 328:501–504.

700 56. Peters JM, Mooney RA, Grass JA, Jessen ED, Tran F, Landick R. 2012. Rho and NusG suppress
701 pervasive antisense transcription in Escherichia coli. Genes Dev 26:2621–2633.

702 57. Zhang T, Shi XC, Xia Y, Mai L, Tremblay PL. 2019. Escherichia coli adaptation and response to
703 exposure to heavy atmospheric pollution. Sci Rep 9:10879.

704 58. Saxena S, Myka KK, Washburn R, Costantino N, Court DL, Gottesman ME. 2018. Escherichia coli
705 transcription factor NusG binds to 70S ribosomes. Mol Microbiol 108:495–504.

706 59. Wang B, Artsimovitch I. 2021. NusG, an Ancient Yet Rapidly Evolving Transcription Factor. Front
707 Microbiol 11.

708 60. Bailey EJ, Gottesman ME, Gonzalez RL. 2022. NusG-mediated Coupling of Transcription and
709 Translation Enhances Gene Expression by Suppressing RNA Polymerase Backtracking. J Mol Biol
710 434:167330.

711 61. Rodríguez-Verdugo A, Tenaillon O, Gaut BS. 2016. First-Step Mutations during Adaptation Restore
712 the Expression of Hundreds of Genes. Mol Biol Evol 33:25–39.

713 62. LaCroix RA, Sandberg TE, O'Brien EJ, Utrilla J, Ebrahim A, Guzman GI, Szubin R, Palsson BO, Feist
714 AM. 2015. Use of Adaptive Laboratory Evolution To Discover Key Mutations Enabling Rapid
715 Growth of Escherichia coli K-12 MG1655 on Glucose Minimal Medium. Appl Environ Microbiol
716 81:17–30.

717 63. Utrilla J, O'Brien EJ, Chen K, McCloskey D, Cheung J, Wang H, Armenta-Medina D, Feist AM,
718 Palsson BO. 2016. Global Rebalancing of Cellular Resources by Pleiotropic Point Mutations
719 Illustrates a Multi-scale Mechanism of Adaptive Evolution. Cell Syst 2:260–271.

720 64. Gao R, Mack TR, Stock AM. 2007. Bacterial Response Regulators: Versatile Regulatory Strategies
721 from Common Domains. Trends Biochem Sci 32:225–234.

722 65. Martínez-Hackert E, Stock AM. 1997. The DNA-binding domain of OmpR: crystal structures of a
723 winged helix transcription factor. Structure 5:109–124.

724 66. Feldheim YS, Zusman T, Speiser Y, Segal G. 2016. The Legionella pneumophila CpxRA two-
725 component regulatory system: new insights into CpxR's function as a dual regulator and its
726 connection to the effectors regulatory network. Mol Microbiol 99:1059–1079.

727 67. Tanner JR, Li L, Faucher SP, Brassinga AKC. 2016. The CpxRA two-component system contributes
728 to Legionella pneumophila virulence. Mol Microbiol 100:1017–1038.

729 68. Arsène F, Tomoyasu T, Bukau B. 2000. The heat shock response of Escherichia coli. Int J Food
730 Microbiol 55:3–9.

731 69. Cheetham ME, Caplan AJ. 1998. Structure, function and evolution of DnaJ: conservation and
732 adaptation of chaperone function. Cell Stress Chaperones 3:28–36.

733 70. Chenoweth MR, Wickner S. 2008. Complex regulation of the DnaJ homolog CbpA by the global
734 regulators σS and Lrp, by the specific inhibitor CbpM, and by the proteolytic degradation of
735 CbpM. J Bacteriol 190:5153–5161.

736 71. Genevaux P, Wawrzynow A, Zylicz M, Georgopoulos C, Kelley WL. 2001. DjlA is a third DnaK co-
737 chaperone of Escherichia coli, and DjlA-mediated induction of colanic acid capsule requires DjlA-
738 DnaK interaction. J Biol Chem 276:7906–7912.

739 72. Dalebroux ZD, Yagi BF, Sahr T, Buchrieser C, Swanson MS. 2010. Distinct roles of ppGpp and DksA
740 in Legionella pneumophila differentiation. Mol Microbiol 76:200–219.

741 73. Kim J-S, Liu L, Fitzsimmons LF, Wang Y, Crawford MA, Mastrogiovanni M, Trujillo M, Till JKA, Radi
742 R, Dai S, Vázquez-Torres A. 2018. DksA–DnaJ redox interactions provide a signal for the activation
743 of bacterial RNA polymerase. Proc Natl Acad Sci 115:E11780–E11789.

744 74. Kim J-S, Liu L, Vázquez-Torres A. 2021. The DnaK/DnaJ Chaperone System Enables RNA
745 Polymerase-DksA Complex Formation in Salmonella Experiencing Oxidative Stress. mBio
746 12:e03443-20.

747 75. Liang J, Faucher SP. 2022. Transcriptomic Adaptation of Legionella pneumophila to Transient
748 Heat Shock. Front Water 4.

749 76. Shi Y, Hong X, Wang C. 2005. The C-terminal (331–376) Sequence of Escherichia coli DnaJ Is
750 Essential for Dimerization and Chaperone Activity: A SMALL ANGLE X-RAY SCATTERING STUDY IN
751 SOLUTION*. J Biol Chem 280:22761–22768.

752 77. Cajo GC, Horne BE, Kelley WL, Schwager F, Georgopoulos C, Genevaux P. 2006. The role of the DIF
753 motif of the DnaJ (Hsp40) co-chaperone in the regulation of the DnaK (Hsp70) chaperone cycle. J
754 Biol Chem 281:12436–12444.

755 78. Obrist M, Milek S, Klauck E, Hengge R, Narberhaus F. 2007. Region 2.1 of the Escherichia coli
756 heat-shock sigma factor RpoH (σ32) is necessary but not sufficient for degradation by the FtsH
757 protease. Microbiology 153:2560–2571.

758 79. Jumper J, Evans R, Pritzel A, Green T, Figurnov M, Ronneberger O, Tunyasuvunakool K, Bates R,
759 Žídek A, Potapenko A, Bridgland A, Meyer C, Kohl SAA, Ballard AJ, Cowie A, Romera-Paredes B,
760 Nikolov S, Jain R, Adler J, Back T, Petersen S, Reiman D, Clancy E, Zielinski M, Steinegger M,
761 Pacholska M, Berghammer T, Bodenstein S, Silver D, Vinyals O, Senior AW, Kavukcuoglu K, Kohli
762 P, Hassabis D. 2021. Highly accurate protein structure prediction with AlphaFold. 7873. Nature
763 596:583–589.

764 80. Varadi M, Anyango S, Deshpande M, Nair S, Natassia C, Yordanova G, Yuan D, Stroe O, Wood G,
765 Laydon A, Žídek A, Green T, Tunyasuvunakool K, Petersen S, Jumper J, Clancy E, Green R, Vora A,
766 Lutfi M, Figurnov M, Cowie A, Hobbs N, Kohli P, Kleywegt G, Birney E, Hassabis D, Velankar S.
767 2022. AlphaFold Protein Structure Database: massively expanding the structural coverage of
768 protein-sequence space with high-accuracy models. Nucleic Acids Res 50:D439–D444.

769 81. Alam A, Bröms JE, Kumar R, Sjöstedt A. 2021. The Role of ClpB in Bacterial Stress Responses and
770 Virulence. Front Mol Biosci 8.

771 82. Doyle SM, Hoskins JR, Wickner S. 2012. DnaK Chaperone-dependent Disaggregation by
772 Caseinolytic Peptidase B (ClpB) Mutants Reveals Functional Overlap in the N-terminal Domain
773 and Nucleotide-binding Domain-1 Pore Tyrosine*. J Biol Chem 287:28470–28479.

774 83. Shih C-J, Lai M-C. 2007. Analysis of the AAA+ chaperone clpB gene and stress-response expression
775 in the halophilic methanogenic archaeon Methanohalophilus portucalensis. Microbiol Read Engl
776 153:2572–2583.

777 84. Kedzierska S, Akoev V, Barnett ME, Zolkiewski M. 2003. Structure and Function of the Middle
778 Domain of ClpB from Escherichia coli. Biochemistry 42:14242–14248.

779 85. Weibezahn J, Schlieker C, Tessarz P, Mogk A, Bukau B. 2005. Novel insights into the mechanism of
780 chaperone-assisted protein disaggregation. Biol Chem 386:739–744.

781 86. Carroni M, Kummer E, Oguchi Y, Wendler P, Clare DK, Sinning I, Kopp J, Mogk A, Bukau B, Saibil
782 HR. 2014. Head-to-tail interactions of the coiled-coil domains regulate ClpB activity and
783 cooperation with Hsp70 in protein disaggregation. eLife 3:e02481.

784 87. Haslberger T, Weibezahn J, Zahn R, Lee S, Tsai FTF, Bukau B, Mogk A. 2007. M domains couple the
785 ClpB threading motor with the DnaK chaperone activity. Mol Cell 25:247–260.

786 88. LaBreck CJ, May S, Viola MG, Conti J, Camberg JL. 2017. The Protein Chaperone ClpX Targets
787 Native and Non-native Aggregated Substrates for Remodeling, Disassembly, and Degradation
788 with ClpP. Front Mol Biosci 4.

789 89. Honoré FA, Méjean V, Genest O. 2017. Hsp90 Is Essential under Heat Stress in the Bacterium
790 Shewanella oneidensis. Cell Rep 19:680–687.

791 90. Morán Luengo T, Kityk R, Mayer MP, Rüdiger SGD. 2018. Hsp90 Breaks the Deadlock of the Hsp70
792 Chaperone System. Mol Cell 70:545-552.e9.

793 91. Thomas JG, Baneyx F. 2000. ClpB and HtpG facilitate de novo protein folding in stressed
794 Escherichia coli cells. Mol Microbiol 36:1360–1370.

795 92. Neunuebel MR, Mohammadi S, Jarnik M, Machner MP. 2012. Legionella pneumophila LidA
796 Affects Nucleotide Binding and Activity of the Host GTPase Rab1. J Bacteriol 194:1389–1400.

797 93. Schoebel S, Cichy AL, Goody RS, Itzen A. 2011. Protein LidA from Legionella is a Rab GTPase
798 supereffector. Proc Natl Acad Sci 108:17945–17950.

799 94. Conover GM, Derré I, Vogel JP, Isberg RR. 2003. The Legionella pneumophila LidA protein: a
800 translocated substrate of the Dot/Icm system associated with maintenance of bacterial integrity.
801 Mol Microbiol 48:305–321.

802 95. Huang L, Boyd D, Amyot WM, Hempstead AD, Luo Z-Q, O'Connor TJ, Chen C, Machner M,
803 Montminy T, Isberg RR. 2011. The E Block motif is associated with Legionella pneumophila
804 translocated substrates. Cell Microbiol 13:227–245.

805 96. Lesnik R, Brettar I, Höfle MG. 2016. Legionella species diversity and dynamics from surface
806 reservoir to tap water: From cold adaptation to thermophily. ISME J 10:1064–1080.

807 97. Mendis N, McBride P, Faucher SP. 2015. Short-term and long-term survival and virulence of
808 legionella pneumophila in the defined freshwater medium Fraquil. PLoS ONE 10:1–17.

809 98. Li L, Mendis N, Trigui H, Faucher SP. 2015. Transcriptomic changes of Legionella pneumophila in
810 water. BMC Genomics 16:637.

811 99. Chen S, Zhou Y, Chen Y, Gu J. 2018. Fastp: An ultra-fast all-in-one FASTQ preprocessor.
812 Bioinformatics 34:i884–i890.

813 100. Deatherage DE, Barrick JE. 2014. Identification of mutations in laboratory-evolved microbes from
814 next-generation sequencing data using breseq, p. 165–188. *In* Sun, L, Shou, W (eds.), Methods in
815 Molecular Biology. Springer New York, New York, NY.

816 101. Langmead B, Wilks C, Antonescu V, Charles R. 2019. Scaling read aligners to hundreds of threads
817 on general-purpose processors. Bioinforma Oxf Engl 35:421–432.

818 102. Langmead B, Salzberg SL. 2012. Fast gapped-read alignment with Bowtie 2. 4. Nat Methods
819 9:357–359.

820 103. R Core Team. 2021. R: A Language and Environment for Statistical Computing. R Foundation for
821 Statistical Computing, Vienna, Austria. https://www.R-project.org/.

822 104. Svec D, Tichopad A, Novosadova V, Pfaffl MW, Kubista M. 2015. How good is a PCR efficiency
823 estimate: Recommendations for precise and robust qPCR efficiency assessments. Biomol Detect
824 Quantif 3:9–16.

825 105. Yuan JS, Wang D, Stewart Jr. CN. 2008. Statistical methods for efficiency adjusted real-time PCR
826 quantification. Biotechnol J 3:112–123.

827 106. Rao C, Benhabib H, Ensminger AW. 2013. Phylogenetic Reconstruction of the Legionella
828 pneumophila Philadelphia-1 Laboratory Strains through Comparative Genomics. PLoS ONE 8.

829 107. De Felipe KS, Glover RT, Charpentier X, Anderson OR, Reyes M, Pericone CD, Shuman HA. 2008.
830 Legionella eukaryotic-like type IV substrates interfere with organelle trafficking. PLoS Pathog
831 4:e1000117.

832 108. Chen J, de Felipe KS, Clarke M, Lu H, Anderson OR, Segal G, Shuman HA. 2004. Legionella
833 Effectors That Promote Nonlytic Release from Protozoa. Science 303:1358–1361.

834 109. Faucher SP, Mueller CA, Shuman HA. 2011. Legionella pneumophila transcriptome during
835 intracellular multiplication in human macrophages. Front Microbiol 2:60.

836 110. Hovel-Miner G, Pampou S, Faucher SP, Clarke M, Morozova I, Morozov P, Russo JJ, Shuman HA,
837 Kalachikov S. 2009. σ S controls multiple pathways associated with intracellular multiplication of
838 Legionella pneumophila. J Bacteriol 191:2461–2473.

839

840

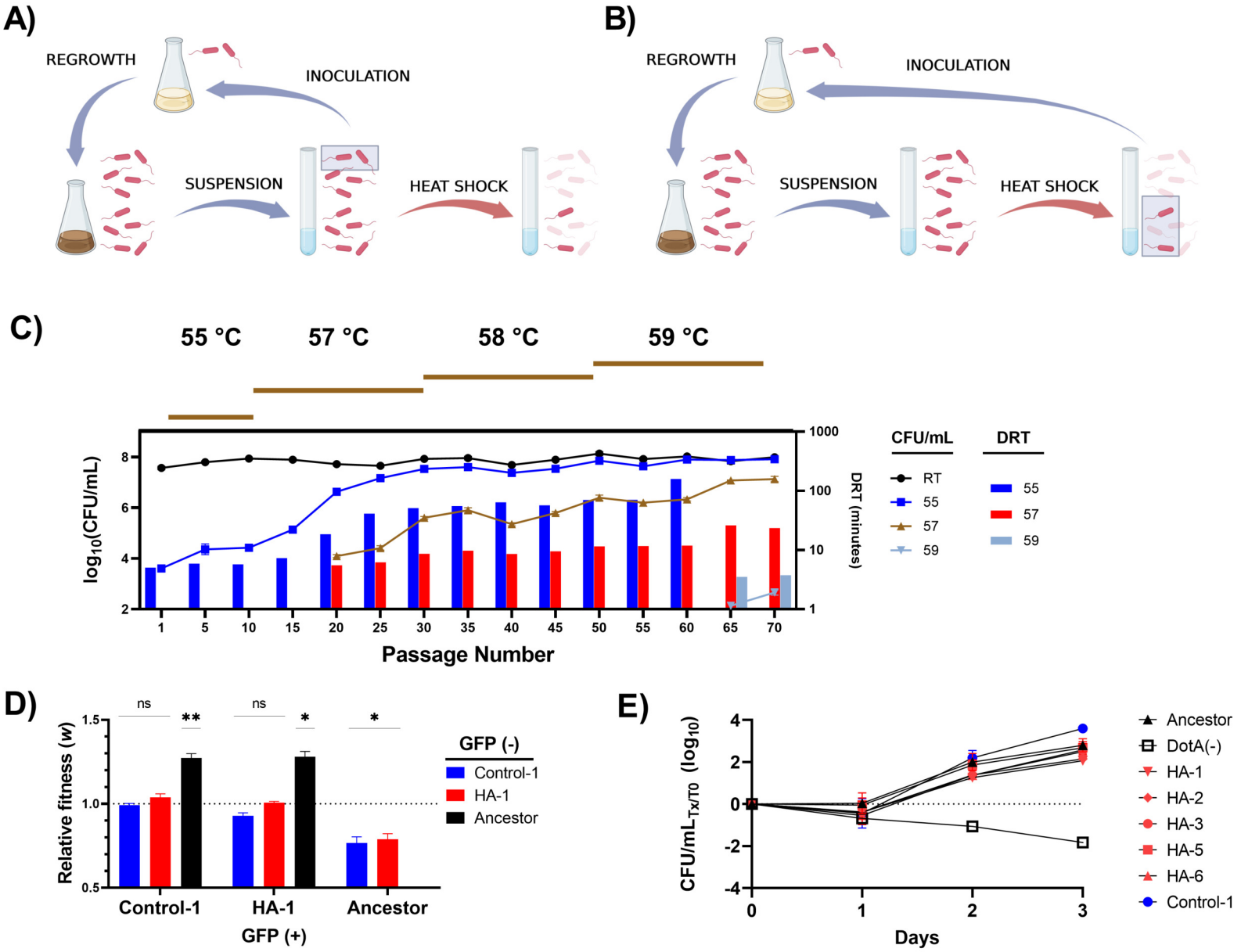
A)
REGROWTH
INOCULATION
SUSPENSION
HEAT SHOCK
B)
REGROWTH
INOCULATION
SUSPENSION
HEAT SHOCK
C)
55 °C
57 °C
58 °C
59 °C
log10(CFU/mL)
DRT (minutes)
Passage Number
CFU/mL
RT
55
57
59
DRT
55
57
59
D)
Relative fitness (w)
ns
**
ns
*
*
Control-1
HA-1
Ancestor
GFP (+)
GFP (-)
Control-1
HA-1
Ancestor
E)
CFU/mL-Tx/T0 (log10)
Days
Ancestor
DotA(-)
HA-1
HA-2
HA-3
HA-5
HA-6
Control-1

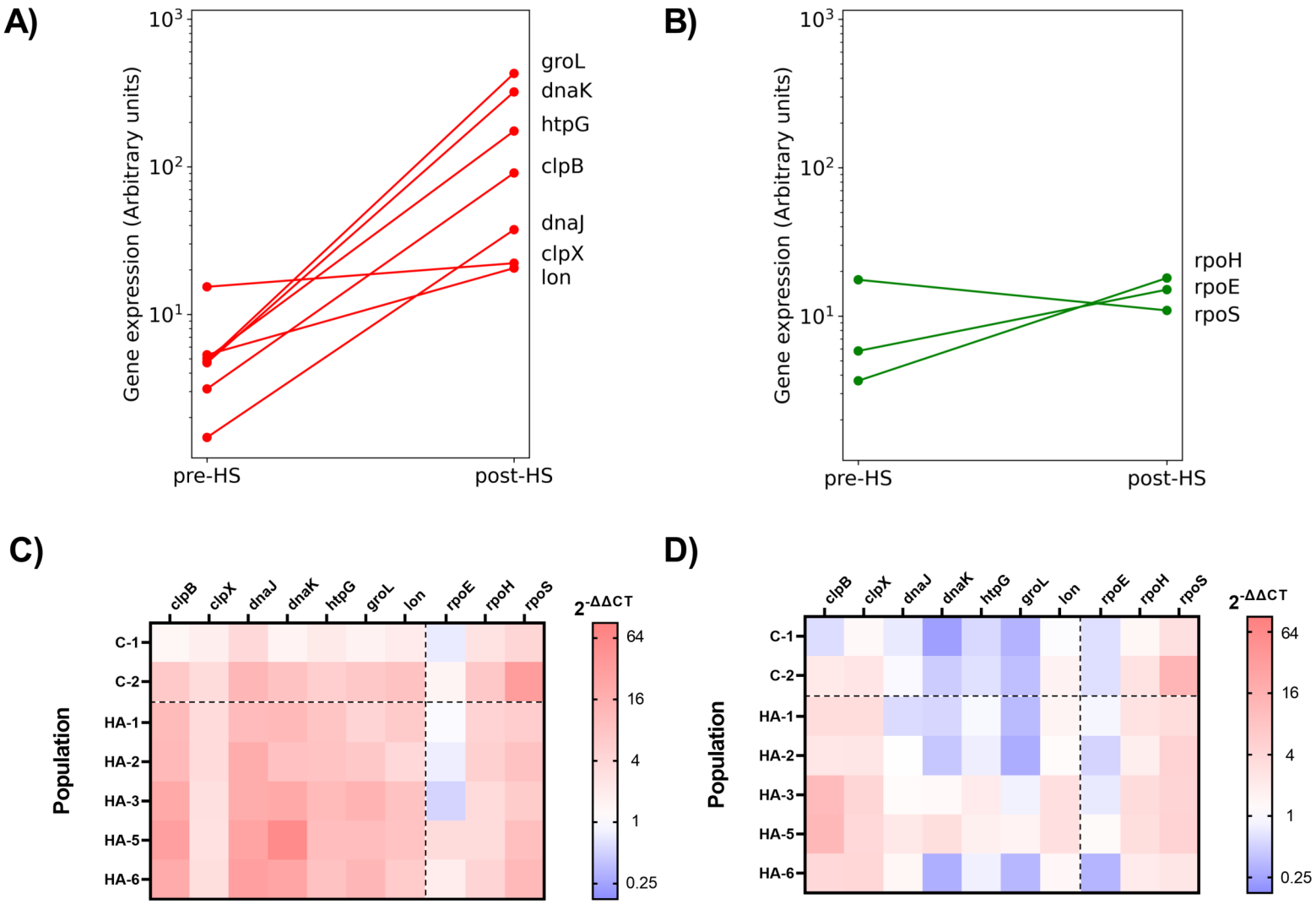
A)
Gene expression (Arbitrary units)
10^3
10^2
10^1
groL
dnaK
htpG
clpB
dnaJ
clpX
lon
pre-HS
post-HS
B)
Gene expression (Arbitrary units)
10^3
10^2
10^1
rpoH
rpoE
rpoS
pre-HS
post-HS
C)
clpB
clpX
dnaJ
dnaK
htpG
groL
lon
rpoE
rpoH
rpoS
Population
C-1
C-2
HA-1
HA-2
HA-3
HA-5
HA-6
$2^{-\Delta\Delta CT}$
64
16
4
1
0.25
D)
clpB
clpX
dnaJ
dnaK
htpG
groL
lon
rpoE
rpoH
rpoS
Population
C-1
C-2
HA-1
HA-2
HA-3
HA-5
HA-6
$2^{-\Delta\Delta CT}$
64
16
4
1
0.25

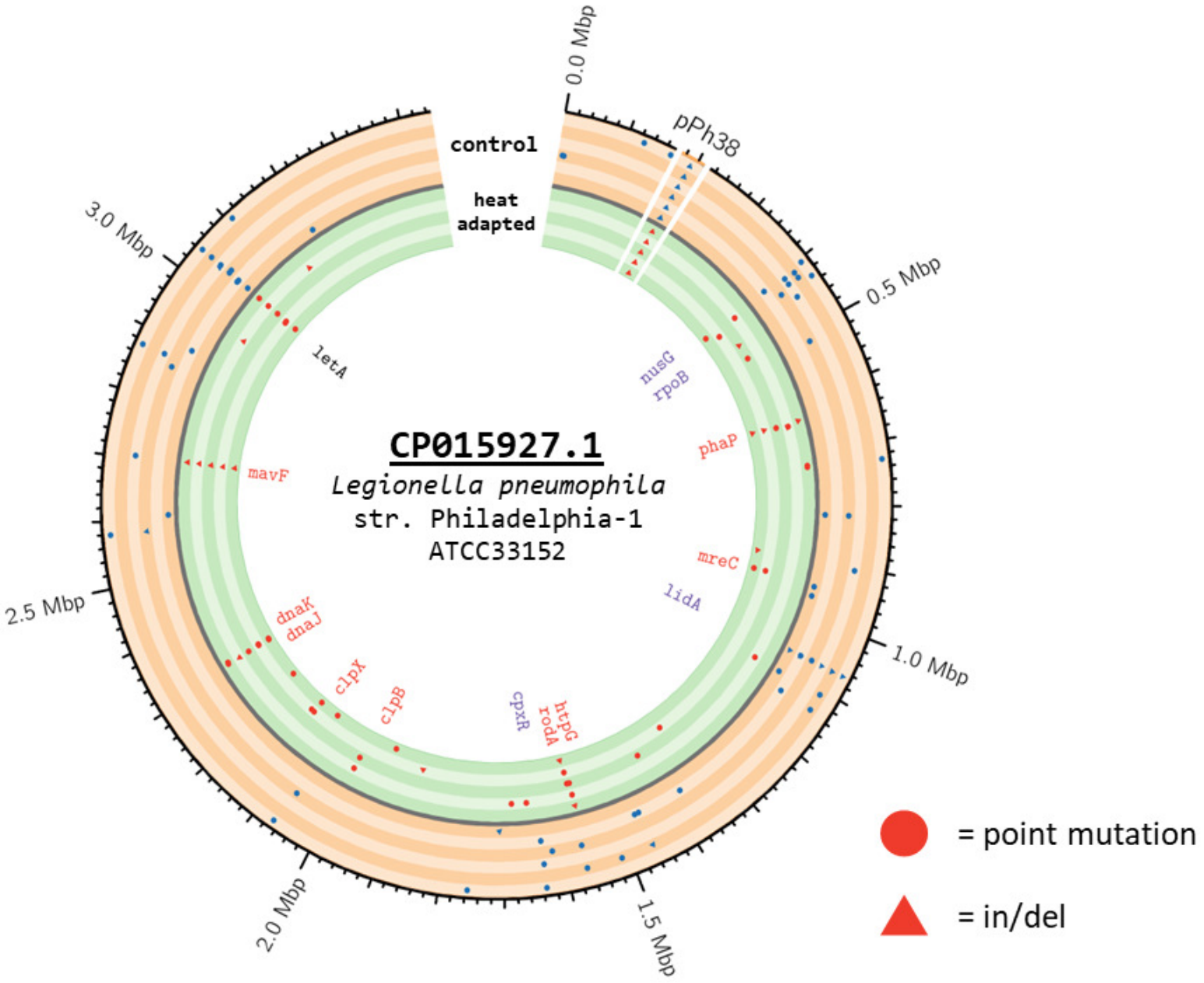
0.0 Mbp
pPh38
control
heat adapted
0.5 Mbp
1.0 Mbp
1.5 Mbp
2.0 Mbp
2.5 Mbp
3.0 Mbp
letA
nusG
rpoB
phaP
mreC
lidA
mavF
dnaK
dnaJ
clpX
clpB
cpxR
htpG
rodA
CP015927.1
Legionella pneumophila
str. Philadelphia-1
ATCC33152
= point mutation
= in/del

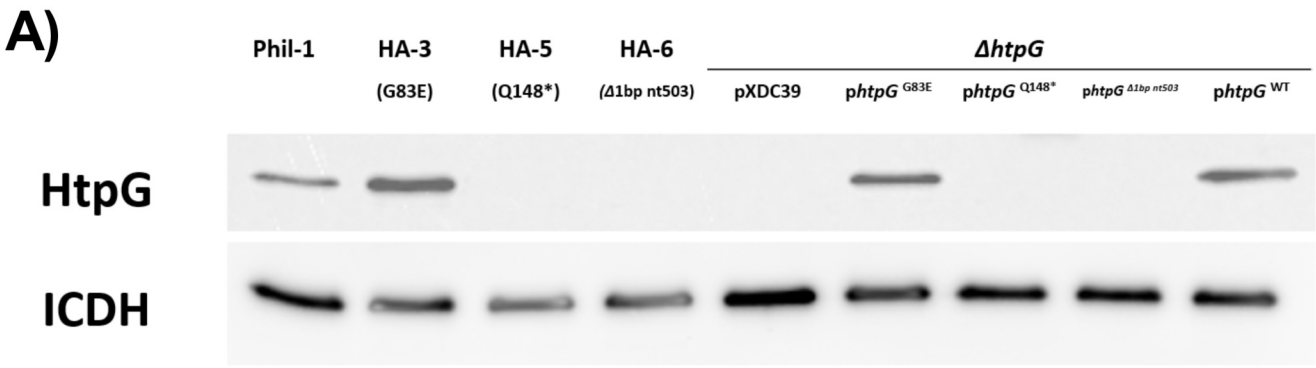
A)
Phil-1
HA-3
(G83E)
HA-5
(Q148*)
HA-6
(Δ1bp nt503)
ΔhtpG
pXDC39
phtpG G83E
phtpG Q148*
phtpG Δ1bp nt503
phtpG WT
HtpG
ICDH

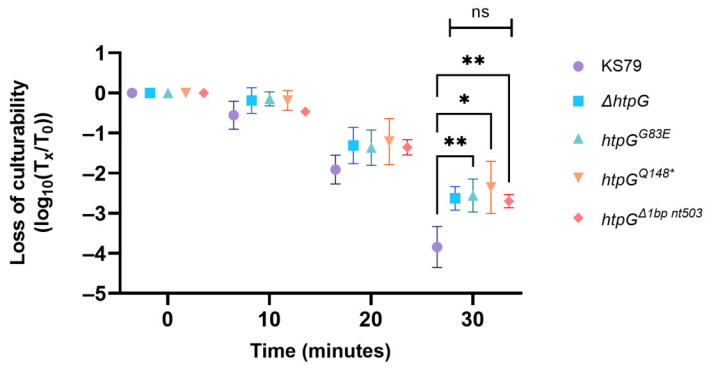
B)
ns
**
*
**
Loss of culturability
(log10(Tx/T0))
Time (minutes)
KS79
ΔhtpG
htpG G83E
htpG Q148*
htpG Δ1bp nt503

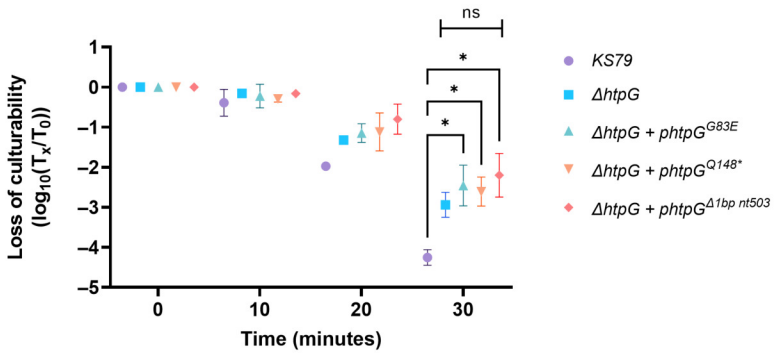
C)
ns
*
*
*
Loss of culturability
(log10(Tx/T0))
Time (minutes)
KS79
ΔhtpG
ΔhtpG + phtpG G83E
ΔhtpG + phtpG Q148*
ΔhtpG + phtpG Δ1bp nt503

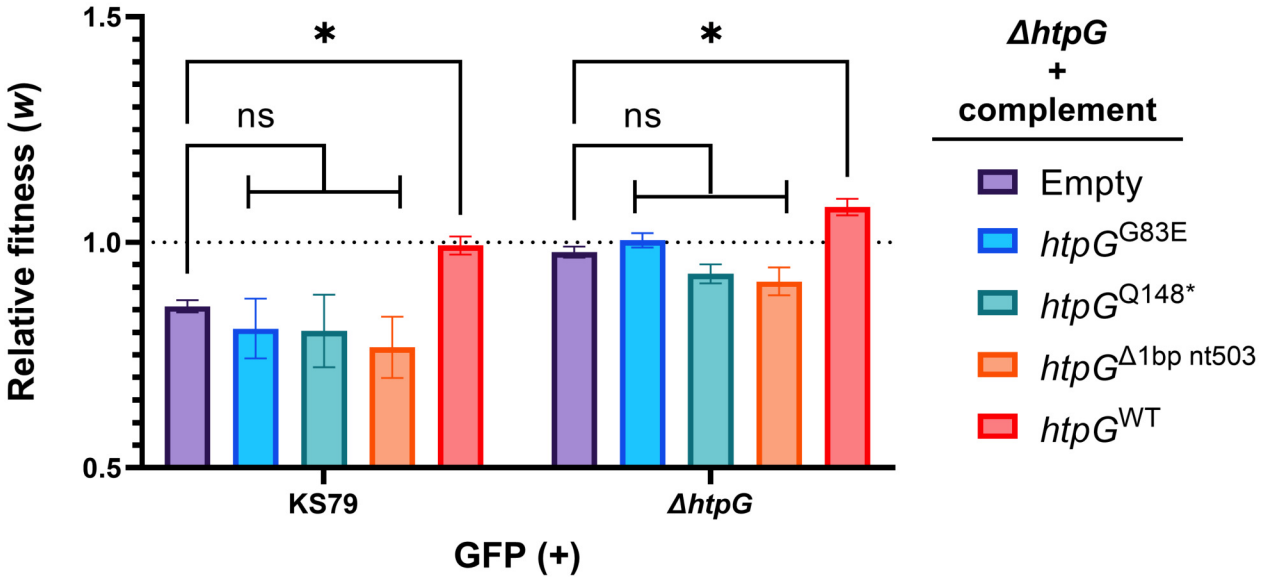
D)
*
*
ns
ns
Relative fitness (w)
KS79
ΔhtpG
GFP (+)
ΔhtpG
+
complement
Empty
htpG G83E
htpG Q148*
htpG Δ1bp nt503
htpG WT